




Peroxioredoxin Asp f3 Is Essential for *Aspergillus fumigatus* To Overcome Iron Limitation during Infection

Victor Brantl,^a Jana M. Boysen,^{b,c} Annie Yap,^d Evgeny Golubtsov,^e Dominik Ruf,^a Thorsten Heinekamp,^f Maria Straßburger,^g Karl Dichtl,^a Hubertus Haas,^d Falk Hillmann,^b  Johannes Wagener^{a,e,h}

^aMax von Pettenkofer-Institut für Hygiene und Medizinische Mikrobiologie, Medizinische Fakultät, LMU München, Munich, Germany

^bEvolution of Microbial Interactions, Leibniz Institute for Natural Product Research and Infection Biology—Hans Knöll Institute, Jena, Germany

^cInstitute of Microbiology, Friedrich Schiller University Jena, Jena, Germany

^dInstitute of Molecular Biology, Medical University of Innsbruck, Innsbruck, Austria

^eInstitut für Hygiene und Mikrobiologie, Julius-Maximilians-Universität Würzburg, Würzburg, Germany

^fDepartment of Molecular and Applied Microbiology, Leibniz Institute for Natural Product Research and Infection Biology—Hans Knöll Institute, Jena, Germany

^gTransfer Group Anti-infectives, Leibniz Institute for Natural Product Research and Infection Biology—Hans Knöll Institute, Jena, Germany

^hDepartment of Clinical Microbiology, School of Medicine, Trinity College Dublin, The University of Dublin, St James's Hospital Campus, Dublin, Ireland

ABSTRACT *Aspergillus fumigatus* is an important fungal pathogen that causes allergic reactions but also life-threatening infections. One of the most abundant *A. fumigatus* proteins is Asp f3. This peroxiredoxin is a major fungal allergen and known for its role as a virulence factor, vaccine candidate, and scavenger of reactive oxygen species. Based on the hypothesis that Asp f3 protects *A. fumigatus* against killing by immune cells, we investigated the susceptibility of a conditional *aspf3* mutant by employing a novel assay. Surprisingly, Asp f3-depleted hyphae were killed as efficiently as the wild type by human granulocytes. However, we identified an unexpected growth defect of mutants that lack Asp f3 under low-iron conditions, which explains the avirulence of the $\Delta aspf3$ deletion mutant in a murine infection model. *A. fumigatus* encodes two Asp f3 homologues which we named Af3I (Asp f3-like) 1 and Af3I2. Inactivation of Af3I1, but not of Af3I2, exacerbated the growth defect of the conditional *aspf3* mutant under iron limitation, which ultimately led to death of the double mutant. Inactivation of the iron acquisition repressor SreA partially compensated for loss of Asp f3 and Af3I1. However, Asp f3 was not required for maintaining iron homeostasis or siderophore biosynthesis. Instead, we show that it compensates for a loss of iron-dependent antioxidant enzymes. Iron supplementation restored the virulence of the $\Delta aspf3$ deletion mutant in a murine infection model. Our results unveil the crucial importance of Asp f3 to overcome nutritional immunity and reveal a new biological role of peroxiredoxins in adaptation to iron limitation.

IMPORTANCE Asp f3 is one of the most abundant proteins in the pathogenic mold *Aspergillus fumigatus*. It has an enigmatic multifaceted role as a fungal allergen, virulence factor, reactive oxygen species (ROS) scavenger, and vaccine candidate. Our study provides new insights into the cellular role of this conserved peroxiredoxin. We show that the avirulence of a $\Delta aspf3$ mutant in a murine infection model is linked to a low-iron growth defect of this mutant, which we describe for the first time. Our analyses indicated that Asp f3 is not required for maintaining iron homeostasis. Instead, we found that Asp f3 compensates for a loss of iron-dependent antioxidant enzymes. Furthermore, we identified an Asp f3-like protein which is partially functionally redundant with Asp f3. We highlight an unexpected key role of Asp f3 and its partially redundant homologue Af3I1 in overcoming the host's nutritional immunity. In addition, we uncovered a new biological role of peroxiredoxins.

KEYWORDS Asp f3, *Aspergillus fumigatus*, peroxiredoxin, iron regulation, virulence

Citation Brantl V, Boysen JM, Yap A, Golubtsov E, Ruf D, Heinekamp T, Straßburger M, Dichtl K, Haas H, Hillmann F, Wagener J. 2021. Peroxioredoxin Asp f3 is essential for *Aspergillus fumigatus* to overcome iron limitation during infection. mBio 12:e00976-21. <https://doi.org/10.1128/mBio.00976-21>.

Editor Jean-Paul Latge, IMBB-FORTH

Copyright © 2021 Brantl et al. This is an open-access article distributed under the terms of the [Creative Commons Attribution 4.0 International license](https://creativecommons.org/licenses/by/4.0/).

Address correspondence to Johannes Wagener, wagenerj@tcd.ie.

Received 31 March 2021

Accepted 9 July 2021

Published 17 August 2021

Several molds in the genus *Aspergillus* are important opportunistic fungal pathogens that cause a broad range of human diseases (1). These include severe invasive infections in immunocompromised patients, so-called invasive aspergillosis (IA; mortality, approximately 30 to 95%), chronic noninvasive (aspergilloma) or semi-invasive colonization of body cavities in healthy or generally immunocompetent individuals, and allergic diseases such as allergic bronchopulmonary aspergillosis (ABPA) and asthma (2–4). In most cases, *Aspergillus fumigatus* is the causative agent (1, 4).

Neutrophils play a major role in the defense against IA (1, 4, 5). Because of this, IA occurs almost exclusively in patients with primary or secondary immunodeficiencies that correlate with neutrophil dysfunction (2, 3). In contrast, allergic diseases result from the exuberant response of the immune system to allergens. Continuing inhalation of *Aspergillus* conidia and hyphal fragments or transient or chronic colonization of the respiratory tract by aspergilli may cause a hypersensitive immune reaction in atopic individuals. This hypersensitivity is typically characterized by IgE and IgG antibodies directed against *Aspergillus* antigens (6, 7). Asp f3 is a highly abundant protein in *A. fumigatus* and was identified, among others, as a major fungal allergen (8, 9). Cutaneous hypersensitivity or positive antibodies in serum against *Aspergillus* antigens, including Asp f3, indicate sensitization, which was proposed as obligatory criterion for diagnosing ABPA (10).

The cellular role of Asp f3 in *A. fumigatus* remained unknown for a long time. In a proteomic approach, Lessing and colleagues showed that Asp f3 is the most upregulated protein in *A. fumigatus* after exposure to hydrogen peroxide (11). Deletion of the encoding gene, *aspf3*, results in complete loss of virulence in a murine infection model (12). Based on its amino acid sequence, Asp f3 is a peroxiredoxin. This biochemical function was later demonstrated with crude extracts of *Aspergillus* in an enzymatic assay (12). The Δ *aspf3* deletion mutant is highly susceptible to hydrogen peroxide and the organic hydroperoxide *tert*-butyl hydroperoxide (*t*-BOOH) (12). It was therefore suggested that Asp f3 has an important function in peroxide detoxification and thereby contributes to virulence, making the pathogen more resistant to reactive oxygen species (ROS) which are released by innate immune cells (e.g., granulocytes) to counter the infection (11, 12). Interestingly, Asp f3 was additionally proposed as a vaccine candidate against IA, since Asp f3-primed CD4⁺ T cells can protect immunosuppressed mice from experimentally induced pulmonary aspergillosis (13, 14).

We recently established a novel killing assay to quantify the antifungal activity of granulocytes (15). In the present study, we used this assay to study the role of Asp f3 for *Aspergillus* to withstand killing by human granulocytes. Unexpectedly, we found that an Asp f3-depleted mutant is not more susceptible to killing than the wild type. In contrast, we detected a severe growth phenotype of Asp f3-lacking mutants under low-iron conditions. Furthermore, we identified an additional peroxiredoxin with partial functional redundancy, which we named Af311 (Asp f3-like 1). Importantly, supplementation with iron restored virulence of the Δ *aspf3* deletion mutant in a murine infection model. Based on our results, we highlight an unexpected key role of Asp f3 and its partially redundant homologue Af311 to overcome nutritional immunity during infection. In addition, we uncover a new biological role of peroxiredoxins.

RESULTS

Asp f3-depleted hyphae are H₂O₂ sensitive but not more efficiently killed by human granulocytes. ROS are of central importance for the host defense against invasive *Aspergillus* infections. This is evidenced by that fact that patients with chronic granulomatous disease (CGD), a hereditary inability of immune cells to produce various ROS, are at high risk for invasive aspergillosis (16). However, it remains controversial whether ROS directly kill the pathogens or indirectly mediate the immune defense, e.g., by promoting neutrophil degranulation and extracellular trap formation (5). The Δ *aspf3* deletion mutant is one of very few *A. fumigatus* mutants described that showed both increased susceptibility to ROS and avirulence in a murine infection model (12). To study the role of human granulocytes in inactivating *A. fumigatus* that lacks the

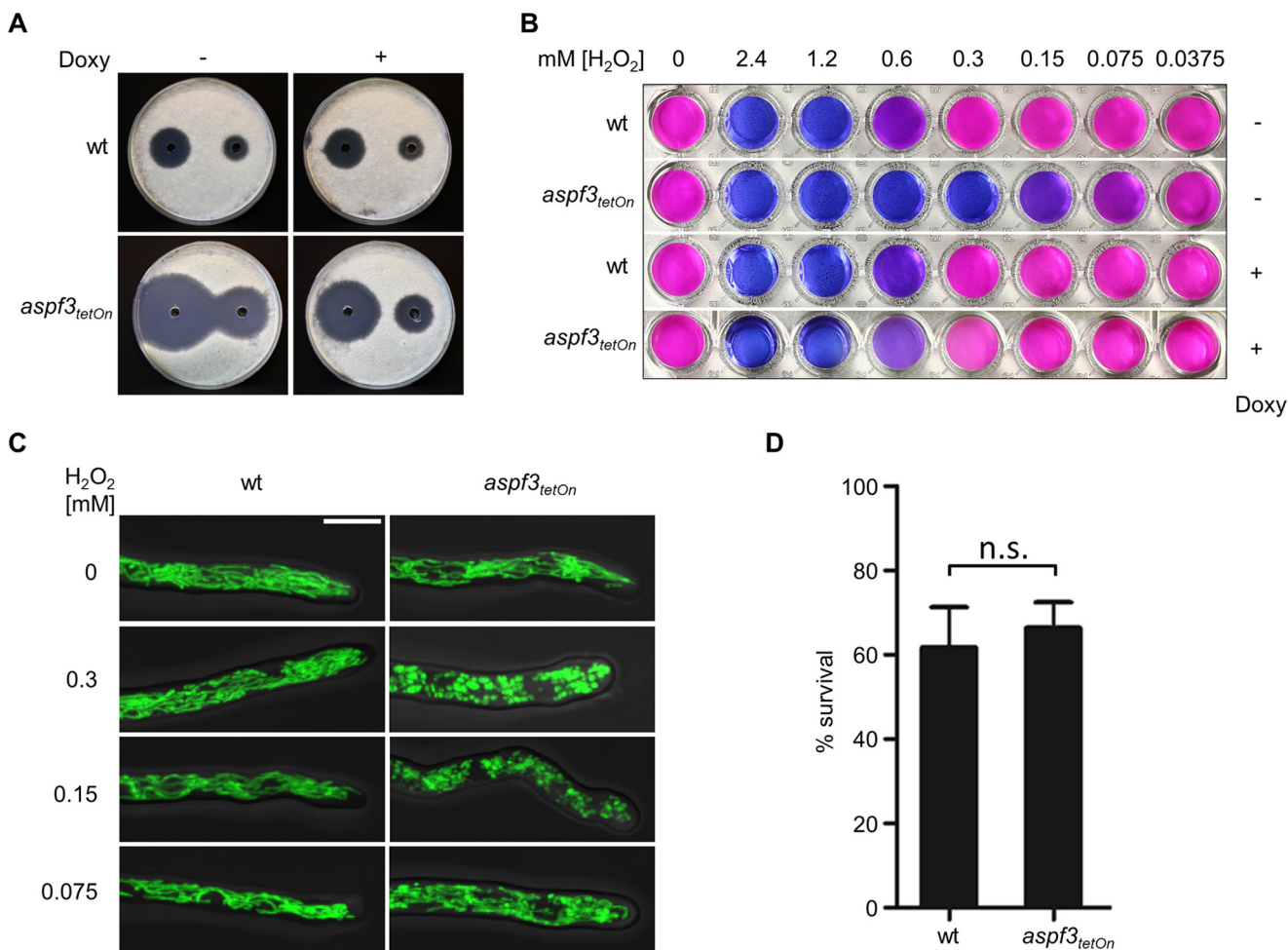


FIG 1 An Asp f3-depleted mutant is hypersensitive to hydrogen peroxide but is not more effectively killed by human granulocytes. (A) Conidia (4×10^5) of the indicated strains were spread on AMM agar plates. When indicated, medium was supplemented with doxycycline ($7.5 \mu\text{g ml}^{-1}$; Doxy). Fifty microliters of 300 mM (left) or 100 mM (right) H₂O₂ was applied in the punch holes of each agar plate. Images were taken after 30 h of incubation at 37°C. (B) Conidia (1.5×10^4) of the indicated strains were inoculated in 100 μl RPMI 1640 per well in a 96-well plate and incubated at 37°C with 5% CO₂. After 10 h, 100 μl medium supplemented with resazurin and, when indicated, H₂O₂ was added to a final concentration of 0.002% (wt/vol) resazurin and the indicated final concentration of H₂O₂. The plate was then incubated for another 24 h at 37°C with 5% CO₂. (C) Conidia of the indicated strains expressing mitochondrion-targeted GFP (mtGFP) were inoculated in RPMI 1640 and incubated at 37°C with 5% CO₂. After 10 h, medium was supplemented with the indicated H₂O₂ concentrations. After 2 h of incubation, samples were fixed and analyzed with a confocal laser scanning microscope. The depicted representative images are overlays of bright-field and GFP fluorescence images of optical stacks covering the entire hypha in focus. Bar, 5 μm (applicable to all images). (D) Conidia of the indicated strains expressing mtGFP were inoculated in RPMI 1640. Human granulocytes (PMNs) were added after 10 h of incubation at 37°C with 5% CO₂. After 2 h coincubation (37°C, 5% CO₂), samples were fixed and stained with calcofluor white. The ratio of vital hyphae (defined as hyphae with tubular or partially tubular mitochondrial morphology in more than 40% of a hyphal volume) was determined as described in Materials and Methods. The data in the graph are based on the results of three independent experiments. Statistical significance (n.s., not significant [$P > 0.05$]) was calculated with a two-tailed unpaired (assuming unequal variances) Student's *t* test. The error bars indicate standard deviations.

peroxide detoxification enzyme Asp f3, we constructed a conditional *aspf3* mutant by replacing the endogenous promoter with a doxycycline-inducible Tet-On promoter system (*aspf3_{tetOn}*). Growth of the wild type and of the induced or repressed *aspf3_{tetOn}* mutant was indistinguishable with respect to germination, growth rate, and formation of conidia (asexual spores) under normal growth conditions (data not shown). However, under repressed conditions, the conditional *aspf3_{tetOn}* mutant exhibited a severe susceptibility to hydrogen peroxide on solid agar and in liquid medium (Fig. 1A and B), very similar to a Δ *aspf3* deletion mutant characterized in previous studies. Induction of the conditional promoter partially rescued the increased hydrogen peroxide susceptibility of the mutant (Fig. 1A and B).

To assess the susceptibility of the *aspf3_{tetOn}* mutant to killing by human granulocytes, we constructed a derivative that constitutively expresses mitochondrion-

targeted green fluorescent protein (mtGFP). This reporter, which we called MitoFLARE, allows visualizing and quantifying of hydrogen peroxide- as well as granulocyte-induced cell death of *Aspergillus* hyphae (15). Hydrogen peroxide readily induced fragmentation of the tubular mitochondrial network, thereby clearly indicating the increased ROS susceptibility of the conditional *aspf3_{tetOn}* mutant under repressed conditions compared to the induced strain or to the mtGFP-expressing wild type (Fig. 1C). Next, we analyzed the susceptibility of the *aspf3_{tetOn}* mutant to killing induced by granulocytes isolated from human blood (15). Surprisingly, the *aspf3_{tetOn}* mutant under repressed conditions was not more prone to granulocyte-induced killing than the wild type (Fig. 1D).

Unexpected growth phenotype under low-iron conditions. Due to its drastically increased susceptibility to peroxides, we expected the conditional *aspf3_{tetOn}* mutant under repressed conditions to be significantly more sensitive to killing by human granulocytes. We therefore attempted to confirm our result in an independent assay that relies on measuring the metabolic activity of the surviving fungi after killing by granulocytes with a colorimetric assay (e.g., see references 17–20). To this end, we inoculated conidia of the wild type and the *aspf3_{tetOn}* strain under inducing and noninducing conditions in RPMI 1640 medium and incubated the respective well plates at 37°C overnight to obtain *Aspergillus* hyphae for exposing to granulocytes. Even though carbonate-buffered RPMI 1640 medium was used, the well plate was incubated at an atmospheric carbon dioxide concentration. This condition unveiled a growth defect (granulocyte independent) of the *aspf3_{tetOn}* mutant under repressed conditions (Fig. 2A).

Apparently, the alkalization of the medium due to atmospheric carbon dioxide concentration and successive loss of the bicarbonate buffer caused precipitation of media components (Fig. 2A; also, see Fig. S1A in the supplemental material). We therefore tested which essential medium supplement can reconstitute growth of the Asp f3-depleted *Aspergillus* mutant. Of the three tested essential metals, i.e., iron, zinc, and copper, iron (Fe²⁺) showed a striking effect (Fig. S1B). Supplementation of the precipitated RPMI 1640 medium with iron sulfate chelated with EDTA (FeSO₄-EDTA), which keeps iron soluble and bioavailable, apparently fully restored growth (Fig. 2B). To confirm these results, we artificially depleted media from free iron by adding bathophenanthrolinedisulfonic acid (BPS) or lactoferrin, a multifunctional protein with antibacterial and antifungal properties that binds iron. As shown in Fig. S1C and Fig. 2D and E, BPS and 2.5 mg ml⁻¹ lactoferrin from bovine milk significantly inhibited growth of the *aspf3_{tetOn}* mutant under repressed conditions. Very similar results were obtained for a Δ *aspf3* deletion mutant compared to its wild type (Fig. 2D and F). Doxycycline induced the conditional promoter of the *aspf3_{tetOn}* mutant and fully rescued growth but did not affect the susceptibility of the Δ *aspf3* deletion mutant (Fig. 2D and E). Supplementation of the medium with iron, however, fully restored growth of both mutants, the repressed *aspf3_{tetOn}* strain and the Δ *aspf3* strain (Fig. 2G and Fig. S1). This demonstrates that Asp f3 plays an important role in growth of *A. fumigatus* under low-iron conditions.

Identification of an Asp f3 homologue with functional overlap under low-iron but not under oxidative-stress conditions. Asp f3 belongs to the atypical 2-Cys group of peroxiredoxins (12, 21, 22). BLAST searches revealed that *A. fumigatus* encodes two other Asp f3-like (Af31) proteins, Afu5g01440 (Af311) and Afu6g12500 (Af312), both of which remained uncharacterized. All three proteins harbor a conserved redoxin (PF08534) protein family (Pfam) (23) pattern that is not found in any other *A. fumigatus* proteins. The opportunistic pathogenic yeast *Candida albicans* encodes three Asp f3/Af311/Af312 homologues (CaAhp1, CaAhp2, and CaTrp99) and baker's yeast (*Saccharomyces cerevisiae*) only one (ScAhp1). Similar to *A. fumigatus*, other *Aspergillus* species, such as *Aspergillus niger*, *Aspergillus flavus* and *Aspergillus nidulans*, each encode three Asp f3/Af311/Af312 homologues. In all these species, the identified proteins are consistent with the proteins that harbor the conserved redoxin (PF08534) protein family pattern.

Alignments of the identified predicted proteins and analysis of transcription start based on RNA sequencing data (24) revealed that the start sites of translation of Af311,

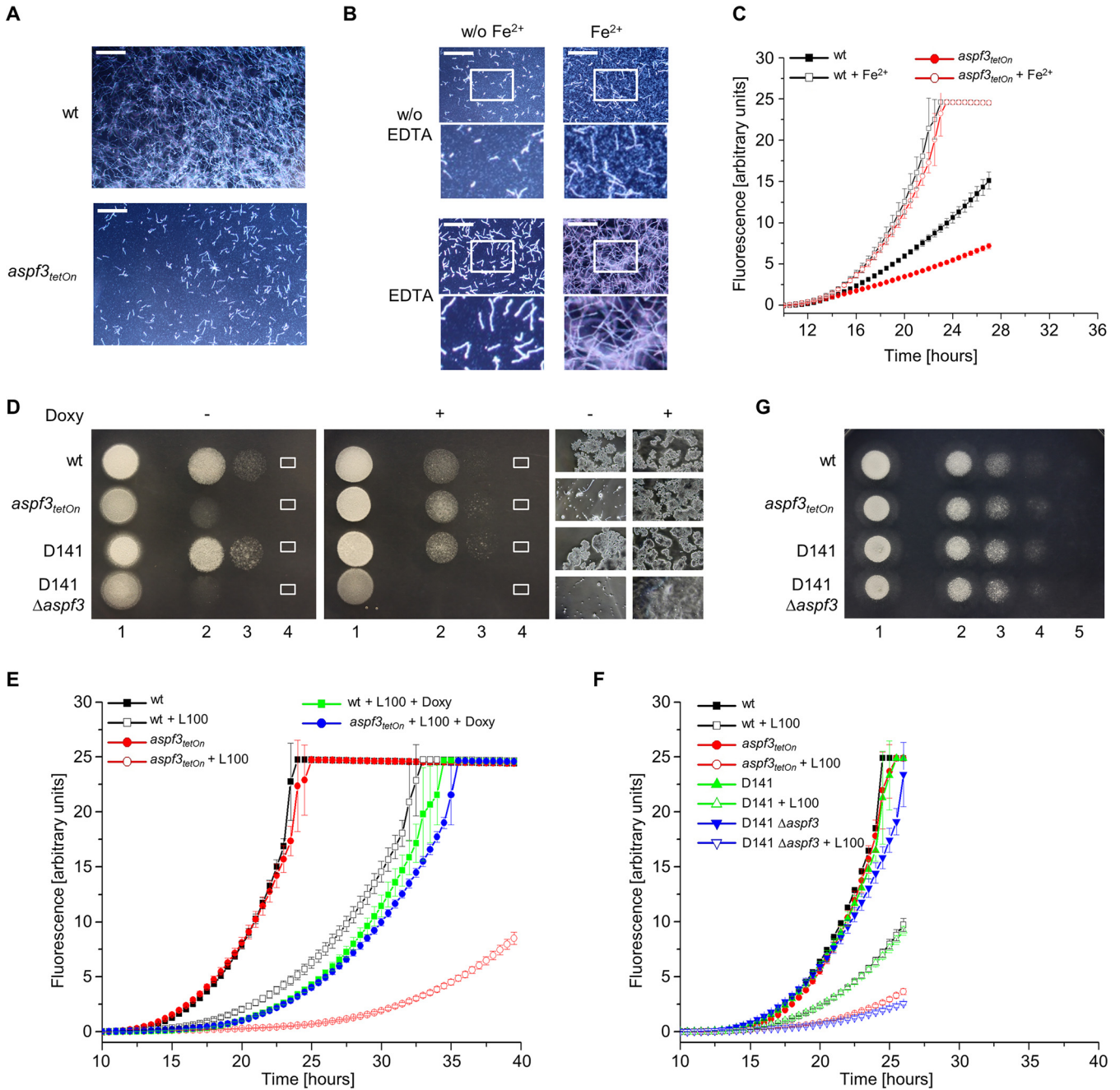


FIG 2 *Asp f3* is important for growth under low-iron conditions. (A and B) Conidia (1.5×10^4) of the indicated strains (A) or of the *aspf3_{tetOn}* strain (B) were inoculated in RPMI 1640 medium supplemented with 0.002% (wt/vol) resazurin per well in a 96-well plate. When indicated, medium was additionally supplemented with or without (w/o) $5 \mu\text{g ml}^{-1}$ FeSO_4 (Fe^{2+}) or $50 \mu\text{g ml}^{-1}$ EDTA. Plates were incubated at 37°C at atmospheric CO_2 concentration, causing partial precipitation of the medium. Representative dark-field images were taken after 10 h. Magnifications of the framed sections of the images are shown in the lower rows. Bars, $250 \mu\text{m}$. (C, E, and F) Conidia (1.5×10^4) of the indicated strains were inoculated in RPMI 1640 medium supplemented with 0.002% (wt/vol) resazurin per well in a 96-well plate. When indicated, medium was additionally supplemented with 100 ng ml^{-1} FeSO_4 (Fe^{2+}), $7.5 \mu\text{g ml}^{-1}$ doxycycline (Doxy), or $100 \mu\text{g ml}^{-1}$ lactoferrin (L100). The plate was then incubated at 37°C with 5% CO_2 . Resorufin fluorescence was documented over time with a microplate reader and plotted in the graphs. The error bars indicate standard deviations for three technical replicates. (D and G) In a series of 10-fold dilutions derived from a starting suspension of 5×10^7 conidia ml^{-1} of the indicated strains, aliquots of $3 \mu\text{l}$ were spotted on peptone agarose plates (1% [wt/vol] agarose, 1% [wt/vol] peptone; pH 7.0) supplemented with 2.5 mg ml^{-1} lactoferrin. When indicated, medium was additionally supplemented with $7.5 \mu\text{g ml}^{-1}$ doxycycline (Doxy). The plate depicted in panel G was additionally supplemented with $5 \mu\text{g ml}^{-1}$ FeSO_4 . Representative images were taken after 30 h (D) or 24 h (G) incubation at 37°C . (D) Magnifications of the framed sections of the images are shown on the right.

Af3l2, and the *A. flavus* proteins encoded by *AFLA_053060* and *AFLA_019280* were most likely incorrectly annotated in the genome database (wrong start codon or splice sites). The corrected protein sequences, including full alignments thereof, are shown in Fig. S2. The tree depicted in Fig. 3A and Fig. S2 shows agglomerative clustering of the

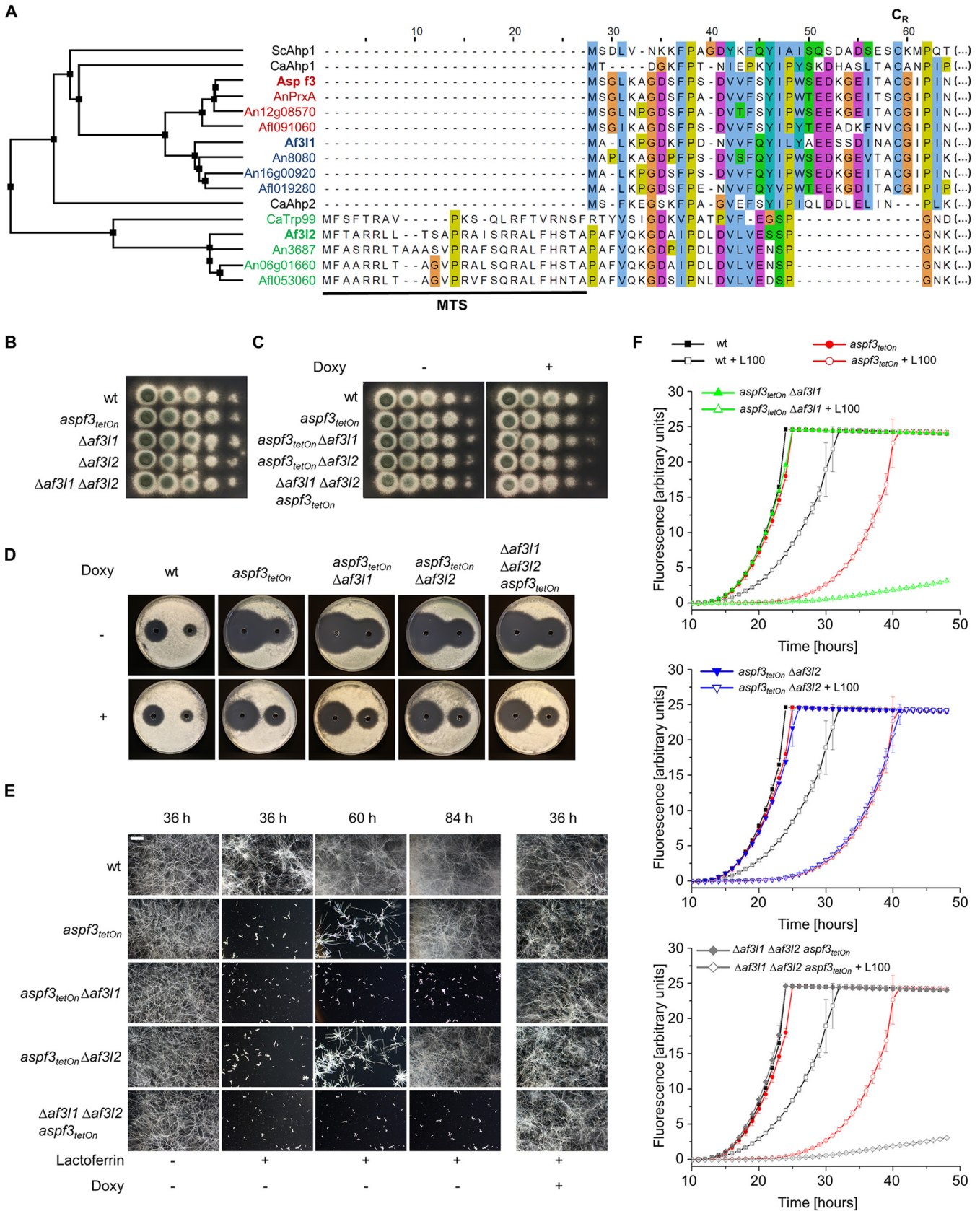
full alignments of Asp f3-like proteins based on average distance and indicates that Af311 and Asp f3 are more similar than Af312 and Asp f3. The *A. nidulans* Asp f3 homologue PrxA (AN8692) was recently characterized and is reported to have a function similar to that previously described for Asp f3 in *A. fumigatus* (25).

In contrast to Asp f3, Af311 and related proteins, Af312 and its homologues (CaTrp99, An3687, and Af1053060) have an N-terminal extension of approximately 25 amino acids preceding the conserved redoxin domain (Fig. 3A). Analysis of the respective sequences with MitoFates (26) indicates that these are mitochondrial targeting signals. Af312 and its homologues are therefore most likely mitochondrial proteins. Interestingly, the Af312-like proteins lack the so-called “resolving” cysteine (C_R) in the N-terminal part of the protein which is highly conserved in the Asp f3- and Af311-like proteins and in ScAhp1 as well as in CaAhp1 (Fig. S2). This cysteine is essential for forming homodimers and for the peroxidase activities of Asp f3 and AnPrxA (12, 25).

We asked whether Af311 and Af312 have functions similar to those of the peroxidases Asp f3 or AnPrxA. We therefore constructed mutants that lack *af311* or *af312*. No growth phenotypes were found under standard growth conditions for both gene deletion mutants (Fig. 3B). Besides this, hydrogen peroxide susceptibility and growth rates under low-iron conditions of the $\Delta af311$ and $\Delta af312$ deletion mutants were similar to those of the wild type (Fig. S3A and B). To check for potential functional redundancy of the enzyme, we constructed double and triple mutants. As shown in Fig. 3C and D, deletion of *af311*, *af312*, or both did not significantly alter growth or the hydrogen peroxide susceptibility of the *aspf3_{tetOn}* mutant under repressed conditions. Significant differences were observed under low-iron conditions. Growth of the *aspf3_{tetOn} Δaf311* double mutant and of the *Δaf311 Δaf312 aspf3_{tetOn}* triple mutant under repressed conditions was drastically reduced compared to that of the *aspf3_{tetOn}* single mutant in the presence of lactoferrin (Fig. 3E and F). Growth reduction under low-iron conditions of the *aspf3_{tetOn} Δaf311* mutant and that of the *Δaf311 Δaf312 aspf3_{tetOn}* mutant were comparable. Deletion of *af312* did not change the low-iron susceptibility of the *aspf3_{tetOn}* mutant under repressed conditions (Fig. 3E and F). Notably, the *aspf3_{tetOn} Δaf311* and the *Δaf311 Δaf312 aspf3_{tetOn}* mutants were constructed independently but showed very similar increase of low-iron susceptibility under repressed conditions compared to the *aspf3_{tetOn}* mutant (Fig. 3E and F). Induction of the Tet-On promoter restored growth of the conditional *aspf3_{tetOn} Δaf311* mutant and the *Δaf311 Δaf312 aspf3_{tetOn}* mutant under low-iron conditions compared to the wild type (Fig. 3E and Fig. S4). This clearly demonstrates that Af311 is partially functionally redundant with Asp f3 under low-iron conditions.

Asp f3 and Af311 are essential for survival under low-iron conditions. Growth of the *aspf3_{tetOn} Δaf311* double mutant under repressed and low-iron conditions was almost abolished. Nevertheless, the *aspf3_{tetOn} Δaf311* conidia were overall able to germinate and form short hyphae, but hyphae then stopped growing (Fig. 3E and 4A). We asked whether these fungi die during germination. The *aspf3_{tetOn} Δaf311* mutant was transformed with a construct expressing mtGFP to visualize mitochondria, in order to quantify viability of individual hyphae (27). Mitochondrial morphology and dynamics of the resulting strain were analyzed over time under repressed conditions (Fig. 4; Videos S1 to S3). As shown in Fig. 4, the germlings still showed dynamic mitochondrial morphology after 12, 24, and 48 h. After 72 h, approximately 70% of the hyphae showed clear evidence of cell death (lysis of mitochondria and release of mtGFP to the cytoplasm, arrest of mitochondrial dynamics, and fading of GFP fluorescence). This indicates that the *aspf3_{tetOn} Δaf311* hyphae are unable to grow but remain alive for an extended period.

Inactivation of the iron acquisition repressor SreA partially compensates for loss of Asp f3 and Af311. Iron uptake of *A. fumigatus* is under the control of a complex regulatory network. The two major regulators of iron homeostasis are SreA and HapX (28, 29). Under iron sufficiency or iron excess conditions, SreA suppresses high-affinity iron uptake and HapX triggers iron detoxification pathways. In contrast, under iron starvation, HapX activates a transcriptional response that results in repression of iron-



consuming pathways and induction of iron uptake. We speculated that the low-iron growth deficiency of *Aspergillus* mutants lacking Asp f3 is related to incomplete derepression of iron acquisition enzymes. Deletion of *sreA* slightly improved the hydrogen peroxide tolerance of wild-type *A. fumigatus* and of the *aspf3_{tetOn}* mutant and the *aspf3_{tetOn} Δaf311* mutant under repressed conditions (Fig. 5A). The growth delay of the wild type observed under low-iron conditions was not improved upon deletion of *sreA* (Fig. 5C). In contrast, deletion of *sreA* significantly improved growth under low-iron conditions of the repressed *aspf3_{tetOn}* and *aspf3_{tetOn} Δaf311* mutants (Fig. 5B and C). However, it did not reach wild-type levels. This suggests either that the low-iron growth deficiency upon depletion of Asp f3 and Af311 is partially related to derepression of iron acquisition or that inactivation of SreA partially compensates for the defect caused by loss of peroxiredoxins indirectly by derepression of iron acquisition or by increasing the conidial iron content. In any case, these data underline a link between peroxiredoxin function and iron homeostasis.

Asp f3 has no major impact on iron homeostasis. Siderophore biosynthesis is vital for growth of *A. fumigatus* under low-iron conditions (28, 29). We speculated that impaired growth of the *aspf3_{tetOn} Δaf311* mutant under low-iron conditions could be linked to a role of the peroxiredoxins in siderophore biosynthesis regulation. We therefore analyzed production of the extracellular siderophores triacetylfusarinine C and fusarinine C and of the intracellular siderophore ferricrocin of the *aspf3_{tetOn}* mutant, the *aspf3_{tetOn} Δaf311* mutant, and the wild type under noninduced and induced conditions. As shown in Fig. 6A, B, and C, we found no significant differences with respect to siderophore biosynthesis in the different strains under repressed conditions. Interestingly, induction of *aspf3* expression with doxycycline seemed to result in a minor increase of fusarinine C synthesis. Nevertheless, this suggests that the growth deficiency of *aspf3_{tetOn}* and *aspf3_{tetOn} Δaf311* mutants under repressed conditions is not related to siderophore biosynthesis. As siderophore biosynthesis is regulated by SreA, these data also indicate that peroxiredoxins do not directly affect SreA activity (see above).

To analyze a potential direct impact of Asp f3 on iron homeostasis during germination, we analyzed transcript levels of iron-regulated genes in conidia and germinating hyphae under low-iron conditions with Northern blot analysis. Altered iron homeostasis, as seen for example in mutants that lack intracellular siderophores (e.g., a *ΔsidA* mutant), was previously shown to cause a characteristic “iron starvation signature” in the conidial transcriptome (30). As shown in Fig. S5A, *hapX* (encoding an iron-regulatory transcription factor, already mentioned above) and *ftrA* (encoding an iron permease involved in reductive iron assimilation) were not upregulated in conidia of the *aspf3_{tetOn}* mutant which were obtained from mycelium on solid agar under repressed conditions. Furthermore, transcript levels of *mirB* (encoding a siderophore transporter) and *ftrA* of the *aspf3_{tetOn}* mutant under repressed conditions were not significantly changed during germination under low-iron conditions (Fig. S5B). Taken together, these data indicate that Asp f3 is not a central regulator of fungal iron homeostasis.

FIG 3 Legend (Continued)

(Af1091060, Af1019280, and Af1053060), *A. niger* (An12g08570, An16g00920, and An06g01660), *S. cerevisiae* (ScAhp1), and *C. albicans* (CaAhp1, CaAhp2, and CaTrp99). The black bar indicates a putative mitochondrial targeting signal (MTS). A conserved resolving cysteine (C_R) is indicated. Sequences of Af311, Af312, Af1019280, and Af1053060 have been corrected taking into account most likely incorrectly annotated start codons or splice sites for the respective sequences in genome databases. Alignment (MAFFT, Clustal color scheme) is based on total protein sequences; the average distance tree was generated with BLOSUM62. The full alignment is available in Fig. S2. (B and C) In a series of 10-fold dilutions derived from a starting suspension of 5×10^7 conidia ml⁻¹ of the indicated strains, aliquots of 3 μl were spotted on AMM agar plates. When indicated, medium was supplemented with 7.5 μg ml⁻¹ doxycycline (Doxy). Representative images were taken after 30 h of incubation at 37°C. (D) Conidia (4×10^5) of the indicated strains were spread on AMM agar plates. When indicated, medium was supplemented with doxycycline (7.5 μg ml⁻¹; Doxy). Fifty microliters of 300 mM (left) or 100 mM (right) H₂O₂ was applied in the punch holes of each agar plate. Images were taken after 30 h of incubation at 37°C. (E and F) Conidia (1.5×10^3 [E] or 1.5×10^4 [F]) of the indicated strains were inoculated in RPMI 1640 medium supplemented with 100 ng ml⁻¹ FeSO₄ per well in 96-well plates. For panel F, medium was additionally supplemented with 0.002% (wt/vol) resazurin. When indicated, medium was additionally supplemented with 100 μg ml⁻¹ lactoferrin (L100) or 7.5 μg ml⁻¹ doxycycline (Doxy). Plates were then incubated at 37°C with 5% CO₂. (E) After the indicated incubation time, representative dark-field images were taken. Bar, 250 μm (applicable to all images). (F) Resorufin fluorescence was documented over time with a microplate reader and plotted in the graph. The error bars indicate standard deviations for three technical replicates.

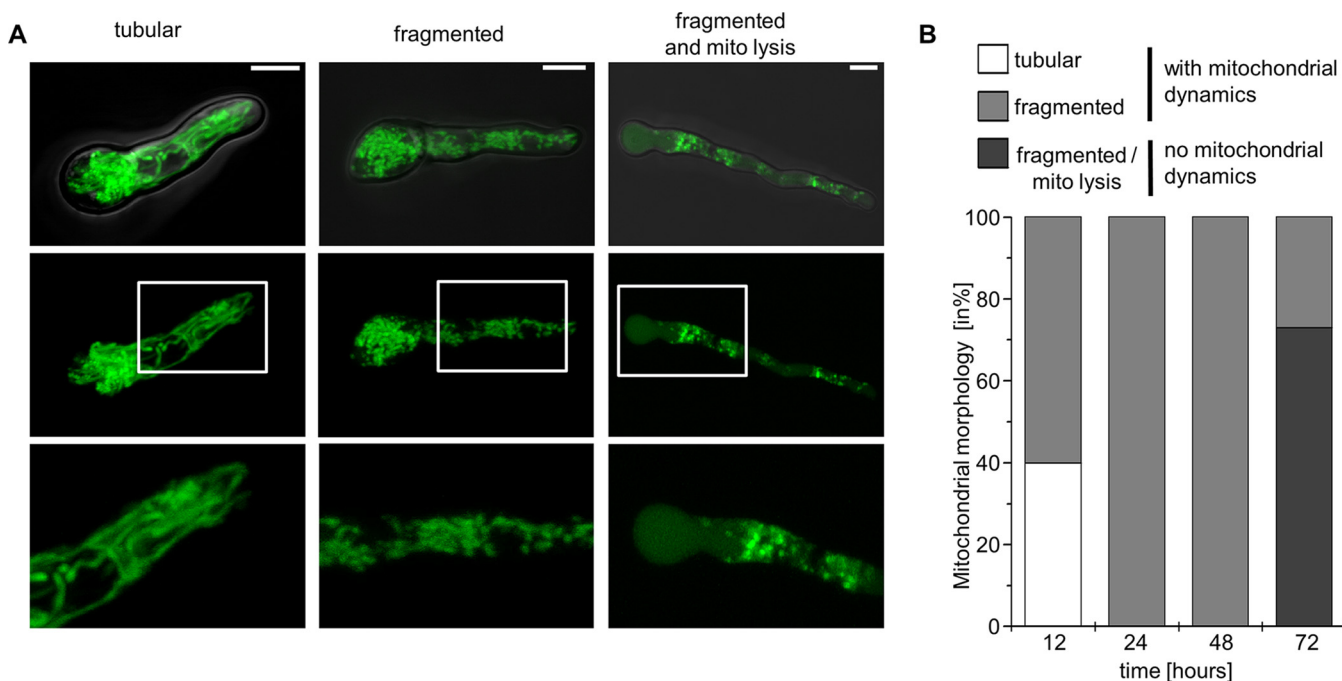


FIG 4 *Asp f3* and *Af311* are essential for survival under iron-limited conditions. (A and B) Conidia of the *aspf3_{tetOn} Δaf311* mutant expressing mitochondrion-targeted GFP (mtGFP) were inoculated in RPMI 1640 supplemented with 100 ng ml⁻¹ FeSO₄ and 200 μg ml⁻¹ lactoferrin under repressed conditions (no doxycycline). Samples were incubated at 37°C with 5% CO₂ and then analyzed with a laser scanning microscope. (A) Representative GFP fluorescence images of hyphae with tubular (left) and fragmented (middle and right) mitochondrial morphology after 12 h, 24 h, and 72 h of incubation, respectively. The hypha on the right shows cytosolic fluorescence, which indicates disruption of mitochondrial integrity (mito lysis) and release of mtGFP to the cytosol. Depicted are images of optical stacks covering the entire hyphae in focus (middle row), magnifications of the framed sections therein (bottom row), and overlays of bright-field and GFP fluorescence images (top row). Bars, 5 μm. (B) The viability of 100 individual hyphae per time point was analyzed in independent samples after 12, 24, 48, and 72 h of incubation based on the mitochondrial morphology and dynamics. Hyphae which exhibited a tubular or fragmented mitochondrial morphology with mitochondrial dynamics were considered alive. Hyphae which exhibited a fragmented mitochondrial morphology without mitochondrial dynamics with or without cytosolic fluorescence or no fluorescence were considered dead.

Expression of *aspf3* is responsive to iron availability. Because of the unexpected low-iron growth phenotype of the *aspf3* mutant, we investigated whether *aspf3* expression is subject to iron regulation at the transcriptional level (Fig. 6B). The analysis of the short-term adaptation from iron starvation to iron sufficiency has previously proven to be a highly sensitive tool for identifying iron-dependent regulation (31, 32). The *A. fumigatus* wild type and mutants lacking either *SreA* or *HapX*, which both encode key iron regulators, were cultured under iron starvation for 18 h (-Fe). Subsequently, iron was added, and cultivation was continued for another hour (sFe). While *SreA* transcriptionally represses iron acquisition during iron sufficiency, *HapX* transcriptionally activates iron acquisition and represses iron consumption during iron starvation. Furthermore, *HapX* activates iron-consuming pathways and iron detoxification during short-term adaptation from iron starvation to iron sufficiency (28, 29). As strain and growth condition controls, we analyzed the transcript levels of the genes that encode the siderophore transporter *MirB* (*mirB*, mentioned above) and the heme iron-dependent mycelial catalase *Cat1* (*cat1*). In agreement with previous reports (31, 32), *mirB* showed a decreased transcript level in the *ΔhapX* mutant during iron starvation and was significantly downregulated during short-term adaptation to iron sufficiency, with a slightly increased transcript level in the *ΔsreA* mutant. In contrast, *cat1* expression was downregulated in a *HapX*-dependent manner during iron starvation and induced during short-term adaptation from iron starvation to iron sufficiency. Lack of *SreA* caused an increased *cat1* transcript level during the short-term adaptation, which is most likely a result of increased iron acquisition and, consequently, increased activation of *HapX* in this strain.

During iron starvation, the wild type and the mutant strains displayed similar *aspf3* transcript levels. Upon short-term adaptation to iron sufficiency, the *aspf3* transcript

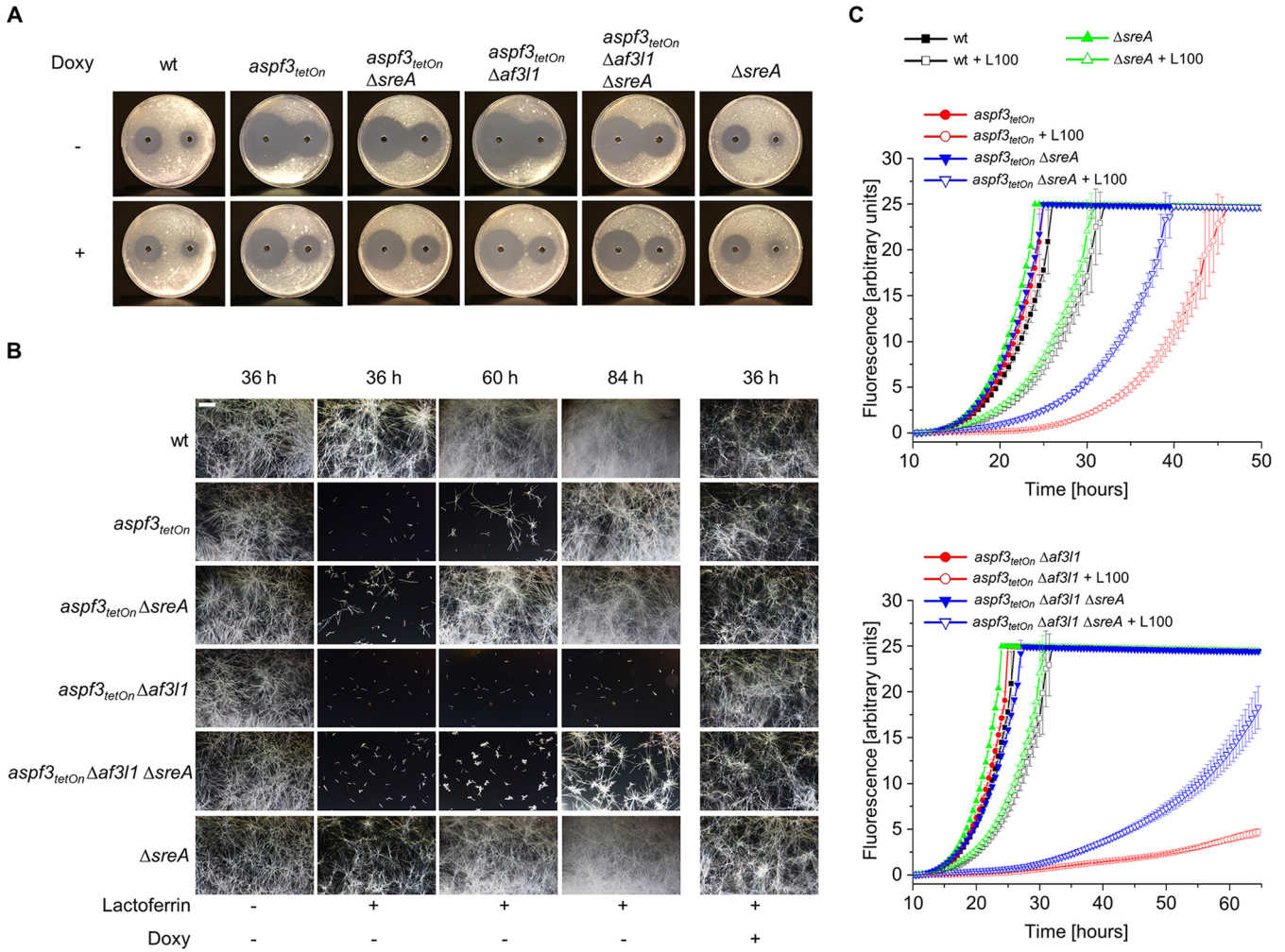


FIG 5 Deletion of the iron acquisition repressor *sreA* partially compensates for loss of *Asp f3* and *Af311*. (A) Conidia (4×10^5) of the indicated strains were spread on AMM agar plates. When indicated, medium was supplemented with doxycycline ($7.5 \mu\text{g ml}^{-1}$; Doxy). Fifty microliters of 300 mM (left) or 100 mM (right) H_2O_2 was applied in the punch holes of each agar plate. Images were taken after 30 h of incubation at 37°C . (B and C) Conidia (1.5×10^3 [B] or 1.5×10^4 [C]) of the indicated strains were inoculated in RPMI 1640 medium supplemented with 100 ng ml^{-1} FeSO_4 per well in 96-well plates. For panel C, medium was additionally supplemented with 0.002% (wt/vol) resazurin. When indicated, medium was additionally supplemented with $100 \mu\text{g ml}^{-1}$ lactoferrin (L100) or $7.5 \mu\text{g ml}^{-1}$ doxycycline (Doxy). Plates were then incubated at 37°C with 5% CO_2 . (B) After the indicated incubation time, representative dark-field images were taken. Bar, $250 \mu\text{m}$ (applicable to all images). (C) Resorufin fluorescence was documented over time with a microplate reader and plotted in the graph. The error bars indicate standard deviations for three technical replicates.

level decreased slightly in the wild type and was more pronounced in the $\Delta sreA$ mutant, while it was largely unaffected in the $\Delta hapX$ mutant. The enhanced downregulation of *aspf3* during short-term adaptation to iron sufficiency in the $\Delta sreA$ mutant compared to the wild type could be explained by the fact that lack of *SreA* leads to elevated iron uptake, which would then increase the slight iron repression observed in the wild type. The lacking downregulation of *aspf3* in the $\Delta hapX$ mutant indicates that *HapX* is required for repression of *aspf3* during short-term adaptation to iron sufficiency. These data demonstrate that *aspf3* expression is modulated by iron availability at the transcript level and responds to iron availability largely inversely compared to *cat1*.

ROS susceptibility of the repressed *aspf3_{tetOn}* and *aspf3_{tetOn} Δaf311* mutants is further increased under low-iron conditions. Our data indicated that compared to the wild type, *cat1* and *aspf3* are inversely regulated in an iron- and *HapX*-dependent manner. The shift from iron starvation to iron sufficiency caused an increase of *cat1* expression and a decrease of *aspf3* expression. Notably, many antioxidant enzymes, such as the major catalases in *A. fumigatus* (*Cat1* and *Cat2*) and the cytochrome *c*

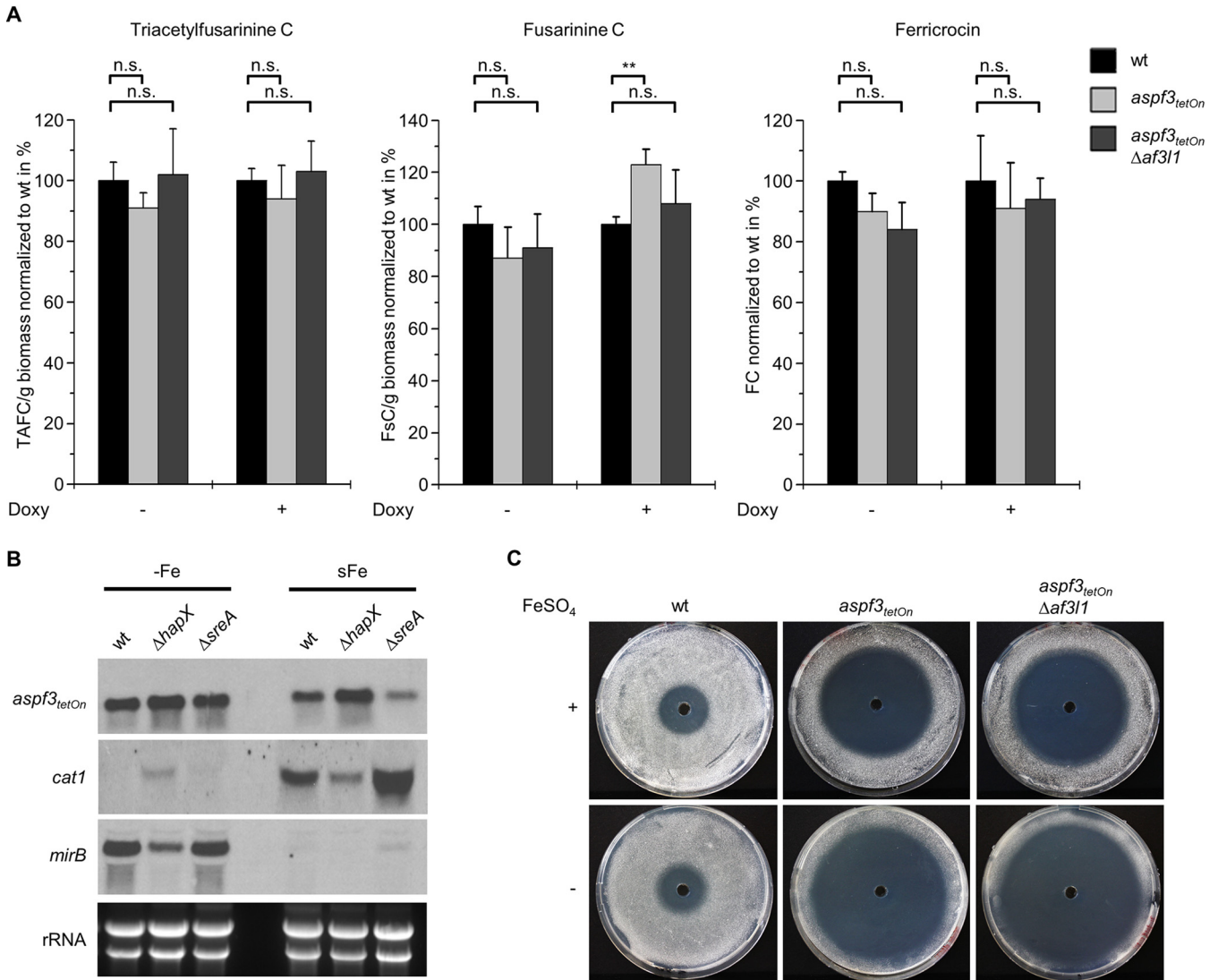


FIG 6 Siderophore biosynthesis is not changed in the *aspf3 af311* mutant, but *aspf3* expression is iron responsive. (A) Production of the extracellular (triacetylfusarinine C and fusarinine C) and intracellular (ferricrocin) siderophores in submerged growth for 18 h at 37°C in a liquid AMM variant as described in Materials and Methods was normalized to biomass and wild type (wt). When indicated, medium was supplemented with doxycycline (10 μg ml⁻¹; Doxy). Statistical significance (n.s., not significant [$P > 0.05$]; **, $P < 0.01$) was calculated with one-way ANOVA with *post hoc* Tukey's HSD test. The error bars indicate standard deviations for three technical replicates. (B) Conidia (1×10^6) of *A. fumigatus* ATCC 46645 (wt) and of the $\Delta hapX$ and $\Delta sreA$ mutants were inoculated in 100 ml of the liquid AMM variant in shake flasks and incubated for 18 h under iron-depleted conditions at 37°C (-Fe). Subsequently, FeSO₄ was added to a final concentration of 0.03 mM, and the cultures were incubated for one more hour at 37°C to monitor short-term adaptation from iron starvation to iron sufficiency (sFe). Total RNA was isolated before (-Fe) and after (sFe) iron addition and subjected to Northern blot analysis with *aspf3*, *cat1*, and *mirB* hybridization probes. Ethidium bromide-stained rRNA is shown as a control for RNA loading and quality. (C) Conidia (1×10^6) of the indicated strains were spread on peptone agarose plates (1% [wt/vol] agarose, 1% [wt/vol] peptone; pH 7.0). When indicated, medium was supplemented with 5 μg ml⁻¹ FeSO₄ (Fe²⁺). Fifty microliters of 100 mM H₂O₂ was applied in the punch holes of each agar plate. Images were taken after 48 h of incubation at 37°C.

peroxidase (Ccp1), functionally depend on iron. We asked whether Asp f3 and Af311 are especially required under low-iron conditions to counter oxidative stress. As shown in Fig. 6C, the hydrogen peroxide inhibition zones of the wild type were indistinguishable on peptone agarose, which is low in iron, and on peptone agarose supplemented with iron sulfate. In marked contrast, the reduced availability iron on the peptone agarose medium drastically increased the hydrogen peroxide susceptibility of the *aspf3_{tetOn}* and *aspf3_{tetOn} Δaf311* mutants under repressed conditions.

Iron restores virulence of the $\Delta asp f3$ mutant in a mammalian infection model.

Our results demonstrated that lactoferrin specifically inhibits growth of the *aspf3_{tetOn}* mutant and the *aspf3_{tetOn} Δaf311* mutant under repressed conditions by sequestering

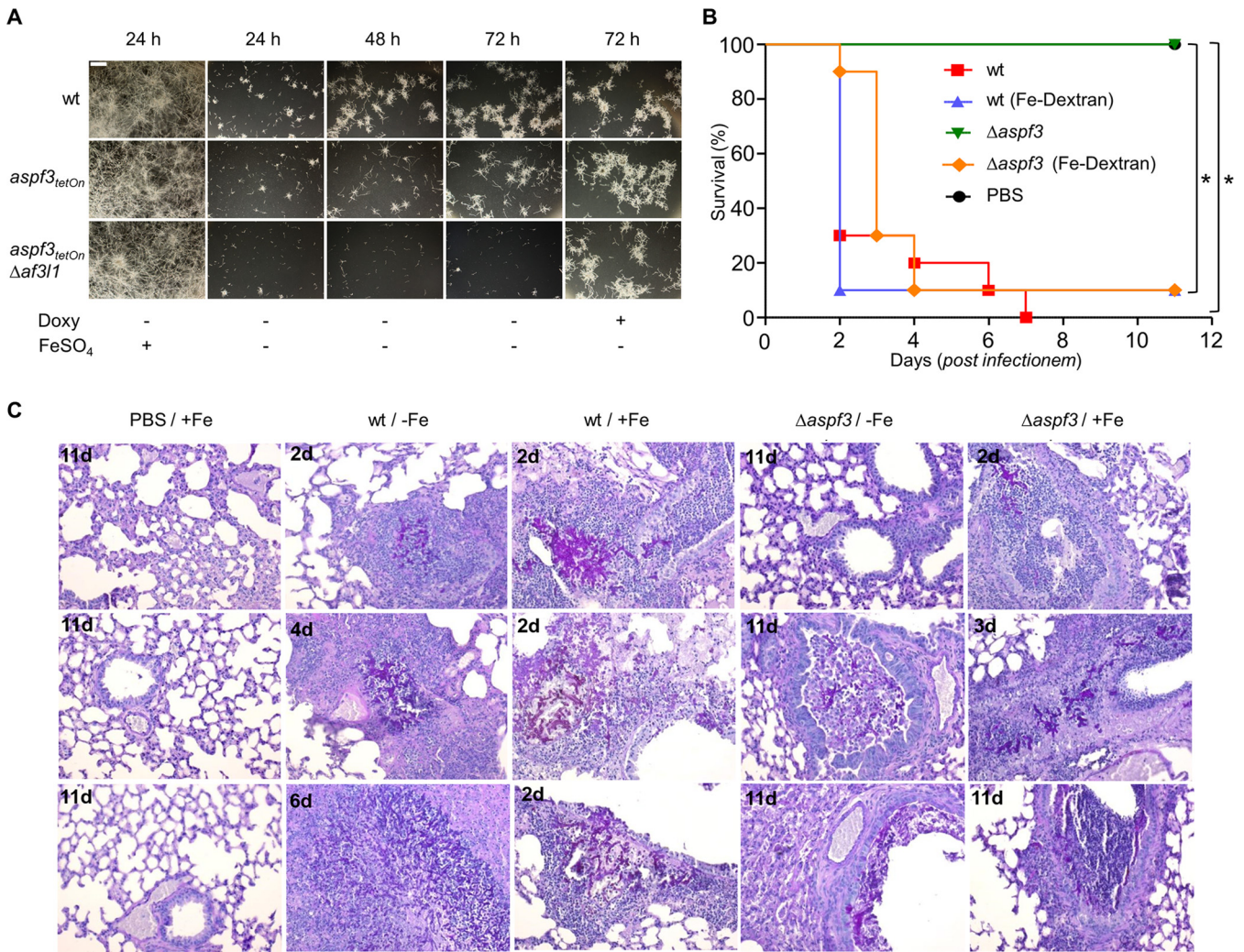


FIG 7 The avirulence of the $\Delta aspf3$ mutant is linked to the iron deprivation in the host. (A) Conidia (1.5×10^3 per well) of the indicated strains were inoculated in 60% (vol/vol) serum in ddH₂O in a 96-well plate. When indicated, medium was supplemented with $50 \mu\text{g ml}^{-1}$ FeSO₄ or $7.5 \mu\text{g ml}^{-1}$ doxycycline (Doxy). Plates were then incubated at 37°C for the indicated times. After the indicated incubation times, representative dark-field images were taken. Bar, 250 μm (applicable to all images). (B) Survival of mice after intranasal infection with conidia of *A. fumigatus* D141 (wt) and the $\Delta aspf3$ mutant. Immunosuppressed mice were left untreated or loaded with iron (iron dextran) prior to intranasal infection with conidia ($n = 10$ per strain/treatment group). A control group ($n = 4$) was infected with PBS as a mock control. The percentage of survivors after each day of infection is shown in the graph. *, $P < 0.001$ (log-rank test and the Gehan-Wilcoxon test). (C) Histology of lungs from mice infected with *A. fumigatus*. Lung sections were stained with periodic acid-Schiff (PAS). The presence of tissue invasive fungal hyphae (magenta) and infiltration of immune cells (purple nuclei) was confirmed in lungs of mice infected with wild-type conidia in the presence (+Fe) or absence (-Fe) of iron and in lung sections infected with the $\Delta aspf3$ strain with Fe. Fungal hyphae and immune cells were rarely found in $\Delta aspf3$ -strain-infected lungs without Fe. Numbers in the upper left corners indicate days postinfection.

available iron. This supports a model where nutritional immunity could be responsible for the previously reported avirulence of the $\Delta aspf3$ deletion mutant in a murine infection model (12). To further substantiate this model, we tested whether the *aspf3*_{tetOn} and the *aspf3*_{tetOn} $\Delta af311$ mutants have specific difficulties growing in serum. Serum is known to be a harsh environment for *Aspergillus* because iron is bound to transferrin and difficult to access (33, 34). As shown in Fig. 7A, growth of the *aspf3*_{tetOn} mutant and, even more so, that of the *aspf3*_{tetOn} $\Delta af311$ mutant in 60% (vol/vol) serum under repressed conditions was significantly reduced compared to that of the wild type. The induction of the conditional promoter with doxycycline restored growth of the two peroxiredoxin mutants to wild-type levels. In agreement with the sequestration of iron being the cause of the reduced growth of the mutants in serum, iron supplementation drastically improved growth of these strains.

This suggests that the avirulence of an $\Delta aspf3$ deletion mutant is primarily linked to the low-iron environment under host infection conditions. To confirm this hypothesis,

we performed a murine infection experiment under conditions that overturn the low-iron conditions in the lungs of a nonneutropenic host. For this, mice were immunosuppressed with cortisone acetate, exposed to high iron levels by intraperitoneal injection of iron dextran, and infected intranasally with conidia of wild-type *A. fumigatus* D141 or of the corresponding $\Delta aspf3$ deletion mutant. For wild-type conidia, such a dose caused a lethal outcome of the infection within 2 to 7 days, independent of iron supplementation. As expected from the previous study, conidia of the $\Delta aspf3$ deletion mutant were avirulent. However, iron supplementation reconstituted their virulence up to wild-type levels (Fig. 7B). Iron-dependent virulence of the $\Delta aspf3$ strain was reflected by histopathological analysis of the lungs of infected mice (Fig. 7C). While tissue invasive hyphae and infiltration of immune cells were frequently found in the wild-type within 2 to 6 days postinfection, tissue invasion was not observed in lungs infected with the $\Delta aspf3$ mutant. Extensive hyphal growth of the mutant was in turn detected after iron supplementation. This shows that the avirulence of the $\Delta aspf3$ mutant is tightly linked to its inability to cope with low-iron conditions and demonstrates that Asp f3 is an essential key player for *A. fumigatus* to overcome iron limitation during infection of a host.

DISCUSSION

Asp f3 is one of the most abundant proteins in *A. fumigatus* and is known for its multifaceted role as an allergen, ROS scavenger, virulence factor, and vaccine candidate (8, 10, 12–14). However, despite being studied for more than 2 decades, the cellular function of Asp f3 remains unknown. A $\Delta aspf3$ deletion mutant is highly susceptible to ROS. It was therefore proposed that the avirulence of the $\Delta aspf3$ deletion mutant in a murine infection model is attributed to more ROS-mediated damage caused by innate immune cells (12, 35, 36). However, we could not observe more efficient killing of the $aspf3_{tetOn}$ hyphae by human granulocytes under repressed conditions compared to wild-type hyphae. This indicates that it is not in the first instance the increased susceptibility to killing by immune cells which is the cause of the avirulence of the $\Delta aspf3$ deletion mutant.

In our study we discovered a new role of the peroxiredoxin Asp f3 and its homologue Af311, which they redundantly exert. The $\Delta aspf3$ deletion mutant and the conditional $aspf3_{tetOn}$ mutant under repressed conditions have severe problems growing under iron-limited conditions. Additional deletion of *af311* significantly reinforces this growth defect. A second Asp f3 homologue, Af312, appears not to be involved in iron homeostasis, as the deletion of the encoding gene did not reinforce the investigated phenotype. This is in agreement with the finding that Af312, in contrast to Asp f3 and Af311, harbors a putative N-terminal mitochondrial targeting signal which presumably guides this protein to a subcellular compartment distinct from that of Asp f3 and Af311.

Homologues of Asp f3 and Af311 are found in other fungal pathogens. Close homologues in *A. nidulans* (AnPrxA), *C. albicans* (CaAhp1), and *S. cerevisiae* (ScAhp1) were shown to have a role in detoxification of ROS, similar to what was previously described for *A. fumigatus* Asp f3 (12, 25, 37, 38). To our knowledge, neither Asp f3 nor any of its homologues in other species has been linked to iron homeostasis or growth under iron-limited conditions. We speculated that Asp f3 and Af311 could be involved in iron homeostasis or siderophore biosynthesis. However, the expression of genes which are typically regulated dependent on the intracellular iron availability, such as those encoding the iron-regulatory transcription factor HapX, the iron permease FtrA, and the siderophore transporter MirB, were not significantly altered in the $aspf3_{tetOn}$ mutant under repressed and low-iron conditions compared to the wild type. Moreover, biosynthesis of the extracellular siderophores triacetylfusarinine C and fusarinine C and of the intracellular siderophore ferricrocin was not significantly changed in mutants lacking Asp f3 and Af311. These results strongly argue against a key regulatory role of Asp f3 and Af311 in maintaining iron homeostasis of *A. fumigatus* under low-iron conditions.

Interestingly, deletion of *sreA*, a gene which encodes the important iron acquisition repressor SreA, partially compensates for the growth defect of the repressed $aspf3_{tetOn}$

and *aspf3_{tetOn} Δaf311* mutants under iron-limited conditions. Surprisingly, ROS tolerance of the *aspf3_{tetOn}* and *aspf3_{tetOn} Δaf311* mutants under repressed conditions was also slightly improved upon deletion of *sreA*. The only partial compensations indicate that the low-iron growth deficiency and the ROS susceptibility are not mediated via SreA hyperactivity in the repressed *aspf3_{tetOn}* and *aspf3_{tetOn} Δaf311* mutants. This is underlined by the fact that siderophore production, which is regulated by SreA (31), was wild type-like in *aspf3_{tetOn}* and *aspf3_{tetOn} Δaf311* mutants. Congruently, it suggests that the ROS susceptibility and the low-iron growth deficiency are linked, as SreA seemingly affects both.

Our data demonstrate that iron depletion with lactoferrin remarkably inhibits germination of *A. fumigatus* conidia which lack Asp f3. Even though lactoferrin was reported to have multiple antimicrobial activities (39), the specific susceptibility of the *aspf3* mutant found in this study is unambiguously linked to the iron sequestration. First, other iron-depleting conditions, e.g., adding the iron chelator BPS, caused a very similar growth defect. Second, supplementation of the lactoferrin-containing medium with iron fully suppressed the growth defect. Lactoferrin is found in excessive amounts in many body fluids, including lung secretions, where it serves as an antimicrobial peptide and sequesters iron (40, 41).

An adequate supply of essential trace elements is crucial for fungal and bacterial pathogens to establish an infection (28, 42). Because of this, metazoa evolved multiple mechanisms to deprive possibly invading microbes from essential trace elements such as iron, a concept which is called nutritional immunity (43). Our results demonstrate that Asp f3 and its homologue Af311 are essentially required to grow and to survive under iron-limited conditions. Importantly, we could show that Asp f3 and Af311 are required to overcome the iron limitation in human serum. Furthermore, we could show that supplementation with iron restores the tissue invasive growth and the virulence of the *Δaspf3* deletion mutant even in the nonneutropenic murine infection model used here. Together, this indicates that the avirulence of the *Δaspf3* deletion is primarily caused by the inability of the mutant to grow under iron-limited conditions, rather than resulting from an increased susceptibility to innate immune cells. It should not be ruled out at this point that *in vivo* innate immune cells, such as neutrophilic granulocytes, may additionally limit the access to iron, e.g., via the well-documented release of lactoferrin (44), or in addition may more efficiently inactivate the mutant because of the increased ROS susceptibility under iron-deprived conditions. In agreement with this model, *aspf3* expression is regulated in a HapX- and iron availability-dependent manner. This makes Asp f3 an important virulence factor which is specifically required to overcome iron-depriving nutritional immunity during infection of the host. In summary, this study highlights for the first time the crucial role of a peroxiredoxin as a virulence factor which is specifically required to overcome iron-depriving nutritional immunity during infection of the host.

What is the mechanism by which Asp f3 and Af311 enable the mold to grow and survive under iron-limited conditions? A recent study performed with baker's yeast revealed that yeast cells that starve produce nontoxic levels of ROS, which results in the unconventional secretion of normally intracellular antioxidant enzymes, including the Asp f3/Af311 homologue ScAhp1 (45). The authors concluded that there is a mechanism whereby antioxidants maintain the cells in a form necessary for growth in case they later return to normal conditions. Interestingly, Asp f3 was also found to be secreted despite lacking a conventional secretion signal in several independent studies (14, 46–48). It is conceivable that *A. fumigatus* and other fungi also rely on antioxidant enzymes to constrain their ROS formation under stressful conditions, such as iron deprivation or germination (49–51). We propose that Asp f3 and Af311 play a major role here. The main antioxidant enzymes, e.g., Cat1 (mycelial catalase), Cat2 (catalase-peroxidase), and Ccp1 (cytochrome c peroxidase), all functionally depend on iron, an essential constituent of their heme groups, and are consequently transcriptionally downregulated during iron starvation to spare iron and to prevent futile protein synthesis (31,

TABLE 1 *A. fumigatus* strains used in this work

Strain or genotype	Relevant genetic modification	Parental strain	Reference
D141			66
$\Delta aspf3$	<i>aspf3::hygro^r</i>	D141	12
AfS35 (wt, if not stated differently)	<i>akuA::loxP</i>	D141	52
<i>aspf3_{tetOn}</i>	<i>aspf3(p)::ptrA-tetOn</i>	AfS35	This work
$\Delta af311$	<i>af311::six-xyIP-β-rec-trpCt-ptrA-six</i>	AfS35	This work
$\Delta af312$	<i>af312::six-xyIP-β-rec-trpCt-ptrA-six</i>	AfS35	This work
$\Delta af311 \Delta af12$	<i>af311::six af312::six-xyIP-β-rec-trpCt-ptrA-six</i>	$\Delta af311$	This work
<i>aspf3_{tetOn} \Delta af311</i>	<i>af311::six-xyIP-β-rec-trpCt-ptrA-six</i>	<i>aspf3_{tetOn}</i>	This work
<i>aspf3_{tetOn} \Delta af312</i>	<i>af312::six-xyIP-β-rec-trpCt-ptrA-six</i>	<i>aspf3_{tetOn}</i>	This work
$\Delta af311 \Delta af312 aspf3tetOn$	<i>aspf3(p)::ptrA-tetOn</i>	$\Delta af311 \Delta af12$	This work
$\Delta sreA$	<i>sreA::six-xyIP-β-rec-trpCt-ptrA-six</i>	AfS35	This work
<i>aspf3_{tetOn} \Delta sreA</i>	<i>sreA::six-xyIP-β-rec-trpCt-ptrA-six</i>	<i>aspf3_{tetOn}</i>	This work
<i>aspf3_{tetOn} \Delta af311 \Delta sreA</i>	<i>af311::six sreA::six-xyIP-β-rec-trpCt-ptrA-six</i>	<i>aspf3_{tetOn} \Delta af311</i>	This work
wt + mtGFP	pCH005	AfS35	15
<i>aspf3_{tetOn}</i> + mtGFP	pCH005	<i>aspf3_{tetOn}</i>	This work
<i>aspf3_{tetOn} \Delta af311</i> + mtGFP	pCH005	<i>aspf3_{tetOn} \Delta af311</i>	This work
ATCC 46645			31
$\Delta sreA$	<i>sreA::hygro^r</i>	ATCC 46645	31
$\Delta hapX$	<i>hapX::hygro^r</i>	ATCC 46645	32
$\Delta sidA$	<i>sidA::hygro^r</i>	ATCC 46645	67

32, 49). Since peroxiredoxins do not depend on heme, Asp f3 and Af311 can step in and could allow the mold to overcome the stress conditions during iron deprivation. In line with this model, we found that (i) even the hyphae of the iron-deprived *aspf3_{tetOn} \Delta af311* mutant under repressed conditions stay alive for several days, reminiscent of the starving yeast cells which depend on antioxidant enzymes to continue to grow (45); (ii) the transcription of *cat1* and that of *aspf3* are inversely regulated depending on iron availability; and (iii) the susceptibility of the repressed *aspf3_{tetOn}* and *aspf3_{tetOn} \Delta af311* mutants to hydrogen peroxide increases even further under low-iron conditions. Future studies will have to explore the cellular function of these peroxiredoxins during iron deprivation in further detail.

MATERIALS AND METHODS

Strains, culture conditions, and chemicals. The strains used and constructed in this study are listed in Table 1. The strains used in this study are derivatives of the *A. fumigatus* strain D141. The $\Delta aspf3$ deletion mutant is a direct derivative of D141 and was described previously (12). The D141 derivative AfS35 is a nonhomologous end joining-deficient strain (52, 53) and was used as progenitor (wild type [wt]) for all mutants constructed in this study. The conditional *aspf3_{tetOn}* mutant was constructed as described before (54). Briefly, the doxycycline-inducible *oIIC-tetOn* promoter cassette derived from pJW128 was inserted before the coding sequence of *aspf3* by double-crossover homologous recombination. Deletion mutants were constructed by replacing the coding region of the respective genes with a self-excising hygromycin B resistance cassette that was obtained from pSK528, essentially as described before (53, 55). Mitochondria were visualized with mitochondrion-targeted green fluorescent protein (mtGFP). To this end, strains were transformed with pCH005, which expresses an N-terminal mitochondrial targeting signal fused to a GFP derivative (sGFP), essentially as described before (56).

Strains were cultured on *Aspergillus* minimal medium (AMM) (57) to harvest conidia if not stated differently. Experiments were performed on or in AMM, RPMI 1640 medium (11835-063; Gibco, Thermo Fisher, Waltham, MA), or peptone medium (pH 7.0) (LP0034B; Oxoid, Thermo Fisher Scientific, Rockford, IL, USA). If not stated differently, experiments performed in RPMI 1640 included incubation with 5% CO₂ and solid media were supplemented with 2% (wt/vol) agar (214030; BD Bioscience, Heidelberg, Germany) or agarose (141098; Serva, Heidelberg, Germany). Resazurin (R7017), paraformaldehyde (158127), bathophenanthrolinedisulfonic acid (BPS; 146617) and calcofluor white (F3543) were obtained from Sigma-Aldrich (St. Louis, MO, USA), hydrogen peroxide (H₂O₂; 8070.2), EDTA (8040.1) and FeSO₄ (P015.1) were obtained from Carl Roth (Karlsruhe, Germany), doxycycline was obtained from Clontech (631311; Mountain View, CA, USA), and Percoll was obtained from GE Healthcare (10253000; Uppsala, Sweden). Lactoferrin from bovine milk was purchased from Ingredia (PEP10LAC02; Ingredia SA, Arras Cedex, France).

MitoFLARE assay with human granulocytes and growth experiment in serum. Viability of *Aspergillus* hyphae after exposure to human granulocytes was analyzed as previously described (15). Briefly, 3 × 10³ conidia of the indicated strains that express mtGFP were inoculated in 300 μl RPMI 1640 per well in μ-Slide 8-well slides (number 80826; Ibidi, Martinsried, Germany). Slides were incubated at

37°C with 5% CO₂. After 10 h of incubation, 1.5×10^6 granulocytes resuspended in 100 μ l RPMI 1640 were added per well. After the indicated incubation time, samples were fixed with 4% (wt/vol) paraformaldehyde for 10 min followed by staining with calcofluor white (1 mg ml⁻¹ in double-distilled water [ddH₂O]) for 10 min. Samples were subsequently washed with phosphate-buffered saline (PBS). In each experiment, 60 hyphae per sample and three samples per condition were analyzed using a fluorescence microscope and a 63 \times objective with oil immersion by an assessor who was blind to sample identity. Samples with different strains were randomly located in each μ -Slide 8-well slide. The calcofluor white and GFP fluorescence and the mitochondrial morphology were analyzed as described before (15). Prior to the blind analysis of an experiment, the killing efficacy of each batch of isolated granulocytes was evaluated with a nonblind wild-type control sample. Experiments where excessive or no significant killing was observed were excluded and not considered in the subsequent statistical analysis (hyphal vitality of wild type after killing for 2 h of <30% or >90%). On that score, of four experiments, one (25%) was excluded because of too-high killing activity and no experiment (0%) because of too-low killing activity. Statistical significance was calculated with a two-tailed unpaired (assuming unequal variances) Student's *t* test posttest. Statistical analysis was done with GraphPad Prism 5 (GraphPad Software, La Jolla, CA, USA).

Granulocytes and serum for the growth inhibition experiment were isolated from the blood of healthy adult volunteers. For serum outgrowth experiments, 1.5×10^3 conidia of the indicated strains were inoculated in 60% (vol/vol) serum in ddH₂O per well in a 96-well plate. The plates were incubated at 37°C for the indicated time. The method for isolating the granulocytes was described before (15). Volunteers gave informed written consent; collection was conducted according to the Declaration of Helsinki and was approved by the Ethics Committee of the LMU München.

Analysis of metabolic activity. The metabolic activity of *Aspergillus* hyphae was analyzed over time with a resazurin reduction assay (58). Conidia (1.5×10^4) were inoculated in 200 μ l RPMI 1640 supplemented with 0.002% (wt/vol) resazurin per well in a 96-well plate (Z707902; TPP, Sigma-Aldrich). Strains were inoculated in triplicate for each experiment. When indicated, medium was additionally supplemented with lactoferrin or FeSO₄. Well plates were sealed with a Breathe-Easy sealing membrane (Z380059; Sigma-Aldrich) and incubated. Plates were subsequently incubated at 37°C with 5% CO₂ and analyzed over time in a BMG Labtech CLARIOstar microplate reader (excitation, 550-15 nm; dichroic mirror, 568.8 nm; emission, 590-20 nm; excitation and detection from the top; BMG Labtech, Ortenberg, Germany).

Microscopy. Fluorescence microscopy to obtain images or to analyze mitochondrial dynamics was performed with a Leica SP5 inverted confocal laser scanning microscope (Leica Microsystems, Mannheim, Germany) equipped with a climate chamber (The Cube & The Box, Life Imaging Services, Switzerland). Quantitative analysis of the killing activity of human granulocytes against *Aspergillus* hyphae was performed with a Leica DM IRB inverted microscope (Leica Microsystems). If not stated differently, 3×10^3 conidia were inoculated in 300 μ l medium per well in a μ -Slide 8-well slide for fluorescence microscopy. Conventional bright- and dark-field images were taken with an EOS 550D digital camera (Canon, Tokyo, Japan) fitted to an Axiovert 25 inverted microscope (Carl Zeiss Microimaging, Göttingen, Germany).

Bioinformatics. Sequences were obtained from FungiDB (59), the *Saccharomyces* Genome Database (60), and the *Candida* Genome Database (61). Alignments were performed with Jalview (62) and MAFFT (multiple alignment using fast Fourier transform); the average distance tree was generated with BLOSUM62.

Murine infection experiment. Prior to infection, *A. fumigatus* D141 and the Δ *aspf3* mutant were grown on malt peptone (MP) agar with 19 g liter⁻¹ malt extract broth (CP75.1; Carl Roth) and 15 g liter⁻¹ agar (5210.2; Carl Roth) with or without 1% (wt/vol) iron dextran (Mediferran; Medistar; 200 mg/ml iron [II] ion) at 37°C for 5 days. Conidia were harvested with sterile PBS with 0.01% (vol/vol) Tween 20 with or without 2% (wt/vol) iron dextran. Conidia were quantified using an automatic cell counter (CASY, model TT; OLS OMNI Life Science, Bremen, Germany). Specific-pathogen-free female outbred CD-1 mice (18 to 20 g; 6 to 8 weeks old) were obtained from Charles River, Germany. Animals were housed under standard conditions in individually ventilated cages and fed normal mouse chow and water *ad libitum*. All animals were cared for in accordance with the European animal welfare regulation, and animal experiments were approved by the responsible federal/state authority and ethics committee in accordance with the German animal welfare act (permit no. 03-009/15). Mice were immunosuppressed with two single doses of 1 g cortisone acetate (C3130-25G, Sigma-Aldrich) per kg of body weight, which were injected intraperitoneally 3 days before and immediately prior to infection with conidia (day 0). Iron loading of mice was achieved by intraperitoneal (i.p.) injection of 20 mg of iron dextran. Subsequently, mice were anesthetized by an intraperitoneal anesthetic combination of midazolam, fentanyl, and medetomidine. Conidia (1×10^6) in 20 μ l PBS were applied to the nares of the mice. Deep anesthesia ensured inhalation of the conidial inocula. Anesthesia was terminated by subcutaneous injection of flumazenil, naloxone, and atipamezole. Infected animals were monitored twice daily to check weight loss and dyspnea. Analysis of the survival data for the murine infection model was assessed with the log-rank test and the Gehan-Wilcoxon test, and *P* values of <0.05 were considered significant.

Histopathological analysis. Lungs of sacrificed mice were fixed in buffered formalin and embedded in paraffin. Sections of 4 μ m were deparaffinized, hydrated in water, and stained with periodic acid-Schiff stain (PAS) using standard protocols. Briefly, sections were oxidized by staining with 1% PA solution for 5 min, incubated with Schiff's reagent for 15 min, and rinsed with tap water between treatments. Counterstaining was carried out with hematoxylin for 30 s, followed by thorough washes with tap water. Stained sections were visualized by light microscopy.

Quantitative analysis of siderophore biosynthesis. For analysis of siderophore production, *A. fumigatus* wild-type and mutant strains were grown for 18 h at 37°C in a liquid *Aspergillus* minimal

medium variant (63) with 20 mM glutamine as the nitrogen source and 1% glucose as the carbon source, omitting addition of iron to generate iron starvation conditions using 10^6 conidia ml^{-1} for inoculation. Production of secreted triacetylfusarinine C and fusarinine C as well of intracellular ferricrocin was quantified from culture supernatants and cell extracts as described previously (64). Produced fungal biomass was harvested by filtration and weighted after freeze-drying for normalization of siderophore production to biomass. Experiments were carried out in triplicate. Statistical significance was calculated with one-way analysis of variance (ANOVA) with a *post hoc* Tukey's honestly significant difference (HSD) test calculator (<https://astatsa.com/>).

Northern blot analysis. To analyze hyphae, conidia of the respective strains were cultured in a liquid *Aspergillus* minimal medium variant (63) with 20 mM glutamine as the nitrogen source and 1% glucose as the carbon source, omitting addition of iron to generate iron starvation conditions. Complete medium (2% [wt/vol] glucose, 0.2% [wt/vol] peptone, 0.1% [wt/vol] yeast extract, 0.1% [wt/vol] Casamino Acids, 7 mM KCl, 2 mM MgSO_4 , 11 mM KH_2PO_4 , and trace elements as described in the recipe for AMM but without iron, with pH adjusted with HCl to 6.5) was used to obtain conidia for RNA isolation and Northern blot analysis. RNA isolation and Northern blot analysis, using 10 μg of extracted RNA, were performed essentially as described previously (65). The digoxigenin-labeled hybridization probes used in this study were generated by PCR. Primers used were 5'-ATGTCTGGACTCAAGGCCG and 5'-TTACAGGTGCTTGAGGACGG for *asp3*, 5'-CCAATGCGGTATGTCCT and 5'-GAGTCATGAGCAGTGGCA for *cat1*, 5'-AAGCCGAGAAAAAGGGG and 5'-AACCAGATGAAGCCCAG for *mirB*, 5'-ATGGCAAAGACGTATTTC and 5'-TCAGACAAGGGATGCTC for *ptrA*, and 5'-TCGGTGGAAAGAGTGCC and 5'-CGAGTCCGTTGGGTATC for *hapX*.

SUPPLEMENTAL MATERIAL

Supplemental material is available online only.

VIDEO S1, AVI file, 4.4 MB.

VIDEO S2, AVI file, 17.6 MB.

VIDEO S3, AVI file, 17.6 MB.

FIG S1, PDF file, 0.3 MB.

FIG S2, PDF file, 0.6 MB.

FIG S3, PDF file, 0.2 MB.

FIG S4, PDF file, 0.2 MB.

FIG S5, PDF file, 0.1 MB.

ACKNOWLEDGMENTS

J.W. conceived the study. J.W. and V.B. wrote the manuscript. H.H. and F.H. reviewed and edited the manuscript. A.Y. and H.H. planned and performed the quantitative analysis of siderophore biosynthesis and Northern blot analyses (Fig. 6A and B and Fig. S5); J.M.B., T.H., M.S., and F.H. planned and performed the murine infection experiment and the histopathological analysis (Fig. 7B and C); all other experiments and analyses were planned and performed by V.B., E.G., D.R., K.D., and J.W. All authors read and authorized the manuscript.

This work was in part supported by the German Research Foundation (J.W., DFG-WA 3016/4-1; J.W. and F.H., DFG-HI 1574/2-1), the Austrian Science Fund (FWF) doctoral program Host Response in Opportunistic Infections (HOROS; W1253 to H.H.), the Verein zur Förderung von Wissenschaft und Forschung an der Medizinischen Fakultät der Ludwig-Maximilians-Universität München e.V., the Förderprogramm für Forschung und Lehre (FöFoLe) of the Medical Faculty of the LMU München, and the Graduate School of Life Sciences (GSLs) at the University of Würzburg.

REFERENCES

1. Sugui JA, Kwon-Chung KJ, Juvvadi PR, Latgé J-P, Steinbach WJ. 2014. *Aspergillus fumigatus* and related species. *Cold Spring Harb Perspect Med* 5:a019786. <https://doi.org/10.1101/cshperspect.a019786>.
2. Kosmidis C, Denning DW. 2015. The clinical spectrum of pulmonary aspergillosis. *Thorax* 70:270–277. <https://doi.org/10.1136/thoraxjnl-2014-206291>.
3. Kousha M, Tadi R, Soubani AO. 2011. Pulmonary aspergillosis: a clinical review. *Eur Respir Rev* 20:156–174. <https://doi.org/10.1183/09059180.00001011>.
4. Brown GD, Denning DW, Gow NAR, Levitz SM, Netea MG, White TC. 2012. Hidden killers: human fungal infections. *Sci Transl Med* 4:165rv13. <https://doi.org/10.1126/scitransmed.3004404>.
5. Espinosa V, Rivera A. 2016. First line of defense: innate cell-mediated control of pulmonary aspergillosis. *Front Microbiol* 7:272. <https://doi.org/10.3389/fmicb.2016.00272>.
6. Tracy MC, Okorie CUA, Foley EA, Moss RB. 2016. Allergic bronchopulmonary aspergillosis. *J Fungi (Basel)* 2:17. <https://doi.org/10.3390/jof2020017>.
7. Page ID, Richardson M, Denning DW. 2015. Antibody testing in aspergillosis—quo vadis? *Med Mycol* 53:417–439. <https://doi.org/10.1093/mmy/myv020>.
8. Hemmann S, Ismail C, Blaser K, Menz G, Cramer R. 1998. Skin-test reactivity and isotype-specific immune responses to recombinant Asp f 3, a major allergen of *Aspergillus fumigatus*. *Clin Exp Allergy* 28:860–867. <https://doi.org/10.1046/j.1365-2222.1998.00329.x>.
9. Hemmann S, Blaser K, Cramer R. 1997. Allergens of *Aspergillus fumigatus* and *Candida boidinii* share IgE-binding epitopes. *Am J Respir Crit Care Med* 156:1956–1962. <https://doi.org/10.1164/ajrccm.156.6.9702087>.
10. Agarwal R, Chakrabarti A, Shah A, Gupta D, Meis JF, Guleria R, Moss R, Denning DW, ABPA complicating asthma ISHAM working group. 2013.

- Allergic bronchopulmonary aspergillosis: review of literature and proposal of new diagnostic and classification criteria. *Clin Exp Allergy* 43:850–873. <https://doi.org/10.1111/cea.12141>.
11. Lessing F, Kniemeyer O, Wozniok I, Loeffler J, Kurzai O, Haertl A, Brakhage AA. 2007. The *Aspergillus fumigatus* transcriptional regulator AfYap1 represents the major regulator for defense against reactive oxygen intermediates but is dispensable for pathogenicity in an intranasal mouse infection model. *Eukaryot Cell* 6:2290–2302. <https://doi.org/10.1128/EC.00267-07>.
 12. Hillmann F, Bagramyan K, Straßburger M, Heinekamp T, Hong TB, Bzymek KP, Williams JC, Brakhage AA, Kalkum M. 2016. The crystal structure of peroxiredoxin Asp f3 provides mechanistic insight into oxidative stress resistance and virulence of *Aspergillus fumigatus*. *Sci Rep* 6:33396. <https://doi.org/10.1038/srep33396>.
 13. Ito JI, Lyons JM, Hong TB, Tamae D, Liu Y-K, Wilczynski SP, Kalkum M. 2006. Vaccinations with recombinant variants of *Aspergillus fumigatus* allergen Asp f 3 protect mice against invasive aspergillosis. *Infect Immun* 74:5075–5084. <https://doi.org/10.1128/IAI.00815-06>.
 14. Diaz-Arevalo D, Bagramyan K, Hong TB, Ito JI, Kalkum M. 2011. CD4+ T cells mediate the protective effect of the recombinant Asp f3-based anti-aspergillosis vaccine. *Infect Immun* 79:2257–2266. <https://doi.org/10.1128/IAI.01311-10>.
 15. Ruf D, Brantl V, Wagener J. 2018. Mitochondrial fragmentation in *Aspergillus fumigatus* as early marker of granulocyte killing activity. *Front Cell Infect Microbiol* 8:128. <https://doi.org/10.3389/fcimb.2018.00128>.
 16. Boyle KB, Stephens LR, Hawkins PT. 2012. Activation of the neutrophil NADPH oxidase by *Aspergillus fumigatus*. *Ann N Y Acad Sci* 1273:68–73. <https://doi.org/10.1111/j.1749-6632.2012.06821.x>.
 17. Bianchi M, Hakkim A, Brinkmann V, Siler U, Seger RA, Zychlinsky A, Reichenbach J. 2009. Restoration of NET formation by gene therapy in CGD controls aspergillosis. *Blood* 114:2619–2622. <https://doi.org/10.1182/blood-2009-05-221606>.
 18. Lee MJ, Liu H, Barker BM, Snarr BD, Gravelat FN, Al Abdallah Q, Gavino C, Baistrocchi SR, Ostapska H, Xiao T, Ralph B, Solis NV, Lehoux M, Baptista SD, Thammahong A, Cerone RP, Kaminsky SGW, Guiot M-C, Latgé J-P, Fontaine T, Vinh DC, Filler SG, Sheppard DC. 2015. The fungal exopolysaccharide galactosaminogalactan mediates virulence by enhancing resistance to neutrophil extracellular traps. *PLoS Pathog* 11:e1005187. <https://doi.org/10.1371/journal.ppat.1005187>.
 19. Loures FV, Röhm M, Lee CK, Santos E, Wang JP, Specht CA, Calich VLG, Urban CF, Levitz SM. 2015. Recognition of *Aspergillus fumigatus* hyphae by human plasmacytoid dendritic cells is mediated by dectin-2 and results in formation of extracellular traps. *PLoS Pathog* 11:e1004643. <https://doi.org/10.1371/journal.ppat.1004643>.
 20. Gazendam RP, van de Geer A, van Hamme JL, Tool ATJ, van Rees DJ, Aarts CEM, van den Biggelaar M, van Alphen F, Verkuijlen P, Meijer AB, Janssen H, Roos D, van den Berg TK, Kuijpers TW. 2016. Impaired killing of *Candida albicans* by granulocytes mobilized for transfusion purposes: a role for granule components. *Haematologica* 101:587–596. <https://doi.org/10.3324/haematol.2015.136630>.
 21. Harper AF, Leuthaeuser JB, Babbitt PC, Morris JH, Ferrin TE, Poole LB, Fetrow JS. 2017. An atlas of peroxiredoxins created using an active site profile-based approach to functionally relevant clustering of proteins. *PLoS Comput Biol* 13:e1005284. <https://doi.org/10.1371/journal.pcbi.1005284>.
 22. Rocha MC, de Godoy KF, Bannitz-Fernandes R, Fabri JHTM, Barbosa MMF, de Castro PA, Almeida F, Goldman GH, da Cunha AF, Netto LES, de Oliveira MA, Malavazi I. 2018. Analyses of the three 1-Cys peroxiredoxins from *Aspergillus fumigatus* reveal that cytosolic Prx1 is central to H2O2 metabolism and virulence. *Sci Rep* 8:12314. <https://doi.org/10.1038/s41598-018-30108-2>.
 23. Mistry J, Chuguransky S, Williams L, Qureshi M, Salazar GA, Sonnhammer ELL, Tosatto SCE, Paladin L, Raj S, Richardson LJ, Finn RD, Bateman A. 2021. Pfam: the protein families database in 2021. *Nucleic Acids Res* 49:D412–D419. <https://doi.org/10.1093/nar/gkaa913>.
 24. Sturm L, Geißel B, Martin R, Wagener J. 2020. Differentially regulated transcription factors and ABC transporters in a mitochondrial dynamics mutant can alter azole susceptibility of *Aspergillus fumigatus*. *Front Microbiol* 11:1017. <https://doi.org/10.3389/fmicb.2020.01017>.
 25. Xia Y, Yu H, Zhou Z, Takaya N, Zhou S, Wang P. 2018. Peroxiredoxin system of *Aspergillus nidulans* resists inactivation by high concentration of hydrogen peroxide-mediated oxidative stress. *J Microbiol Biotechnol* 28:145–156. <https://doi.org/10.4014/jmb.1707.07024>.
 26. Fukasawa Y, Tsuji J, Fu S-C, Tomii K, Horton P, Imai K. 2015. MitoFates: improved prediction of mitochondrial targeting sequences and their cleavage sites. *Mol Cell Proteomics* 14:1113–1126. <https://doi.org/10.1074/mcp.M114.043083>.
 27. Geißel B, Loiko V, Klugherz I, Zhu Z, Wagener N, Kurzai O, van den Hondel C, Wagener J. 2018. Azole-induced cell wall carbohydrate patches kill *Aspergillus fumigatus*. *Nat Commun* 9:3098. <https://doi.org/10.1038/s41467-018-05497-7>.
 28. Misslinger M, Hortschansky P, Brakhage AA, Haas H. 2021. Fungal iron homeostasis with a focus on *Aspergillus fumigatus*. *Biochim Biophys Acta Mol Cell Res* 1868:118885. <https://doi.org/10.1016/j.bbamcr.2020.118885>.
 29. Haas H. 2014. Fungal siderophore metabolism with a focus on *Aspergillus fumigatus*. *Nat Prod Rep* 31:1266–1276. <https://doi.org/10.1039/c4np00071d>.
 30. Wallner A, Blatzer M, Schrettl M, Sarg B, Lindner H, Haas H. 2009. Ferricrocin, a siderophore involved in intra- and transcellular iron distribution in *Aspergillus fumigatus*. *Appl Environ Microbiol* 75:4194–4196. <https://doi.org/10.1128/AEM.00479-09>.
 31. Schrettl M, Kim HS, Eisele M, Kragl C, Nierman WC, Heinekamp T, Werner ER, Jacobsen I, Illmer P, Yi H, Brakhage AA, Haas H. 2008. SreA-mediated iron regulation in *Aspergillus fumigatus*. *Mol Microbiol* 70:27–43. <https://doi.org/10.1111/j.1365-2958.2008.06376.x>.
 32. Schrettl M, Beckmann N, Varga J, Heinekamp T, Jacobsen ID, Jöchl C, Moussa TA, Wang S, Gsaller F, Blatzer M, Werner ER, Niermann WC, Brakhage AA, Haas H. 2010. HapX-mediated adaptation to iron starvation is crucial for virulence of *Aspergillus fumigatus*. *PLoS Pathog* 6:e1001124. <https://doi.org/10.1371/journal.ppat.1001124>.
 33. Hissen AHT, Chow JMT, Pinto LJ, Moore MM. 2004. Survival of *Aspergillus fumigatus* in serum involves removal of iron from transferrin: the role of siderophores. *Infect Immun* 72:1402–1408. <https://doi.org/10.1128/IAI.72.3.1402-1408.2004>.
 34. Petzer V, Wermke M, Tymoszek P, Wolf D, Seifert M, Ovaçin R, Berger S, Orth-Höller D, Loacker L, Weiss G, Haas H, Platzbecker U, Theurl I. 2019. Enhanced labile plasma iron in hematopoietic stem cell transplanted patients promotes *Aspergillus* outgrowth. *Blood Adv* 3:1695–1700. <https://doi.org/10.1182/bloodadvances.2019000043>.
 35. Philippe B, Ibrahim-Granet O, Prévost MC, Gougerot-Pocidallo MA, Sanchez Perez M, Van der Meer A, Latgé JP. 2003. Killing of *Aspergillus fumigatus* by alveolar macrophages is mediated by reactive oxidant intermediates. *Infect Immun* 71:3034–3042. <https://doi.org/10.1128/IAI.71.6.3034-3042.2003>.
 36. Washburn RG, Gallin JI, Bennett JE. 1987. Oxidative killing of *Aspergillus fumigatus* proceeds by parallel myeloperoxidase-dependent and -independent pathways. *Infect Immun* 55:2088–2092. <https://doi.org/10.1128/iai.55.9.2088-2092.1987>.
 37. Lee J, Spector D, Godon C, Labarre J, Toledano MB. 1999. A new antioxidant with alkyl hydroperoxide defense properties in yeast. *J Biol Chem* 274:4537–4544. <https://doi.org/10.1074/jbc.274.8.4537>.
 38. Truong T, Zeng G, Qingsong L, Kwang LT, Tong C, Chan FY, Wang Y, Seneviratne CJ. 2016. Comparative ploid proteomics of *Candida albicans* biofilms unraveled the role of the AHP1 gene in the biofilm persistence against amphotericin B. *Mol Cell Proteomics* 15:3488–3500. <https://doi.org/10.1074/mcp.M116.061523>.
 39. Kell DB, Heyden EL, Pretorius E. 2020. The biology of lactoferrin, an iron-binding protein that can help defend against viruses and bacteria. *Front Immunol* 11:1221. <https://doi.org/10.3389/fimmu.2020.01221>.
 40. Singh PK, Parsek MR, Greenberg EP, Welsh MJ. 2002. A component of innate immunity prevents bacterial biofilm development. *Nature* 417:552–555. <https://doi.org/10.1038/417552a>.
 41. Travis SM, Conway BA, Zabner J, Smith JJ, Anderson NN, Singh PK, Greenberg EP, Welsh MJ. 1999. Activity of abundant antimicrobials of the human airway. *Am J Respir Cell Mol Biol* 20:872–879. <https://doi.org/10.1165/ajrcmb.20.5.3572>.
 42. Gerwien F, Skrahina V, Kasper L, Hube B, Brunke S. 2018. Metals in fungal virulence. *FEMS Microbiol Rev* 42:fux050. <https://doi.org/10.1093/femsre/fux050>.
 43. Nairz M, Weiss G. 2020. Iron in infection and immunity. *Mol Aspects Med* 75:100864. <https://doi.org/10.1016/j.mam.2020.100864>.
 44. Lepanto MS, Rosa L, Paesano R, Valenti P, Cutone A. 2019. Lactoferrin in aseptic and septic inflammation. *Molecules* 24:1323. <https://doi.org/10.3390/molecules24071323>.
 45. Cruz-García D, Brouwers N, Malhotra V, Curwin AJ. 2020. Reactive oxygen species triggers unconventional secretion of antioxidants and Acb1. *J Cell Biol* 219:e201905028. <https://doi.org/10.1083/jcb.201905028>.
 46. Singh B, Oellerich M, Kumar R, Kumar M, Bhadoria DP, Reichard U, Gupta VK, Sharma GL, Asif AR. 2010. Immuno-reactive molecules identified from

- the secreted proteome of *Aspergillus fumigatus*. *J Proteome Res* 9:5517–5529. <https://doi.org/10.1021/pr100604x>.
47. Ramirez-Garcia A, Pellon A, Buldain I, Antoran A, Arbizu-Delgado A, Guruceaga X, Rementeria A, Hernando FL. 2018. Proteomics as a tool to identify new targets against *Aspergillus* and *Scenedosporium* in the context of cystic fibrosis. *Mycopathologia* 183:273–289. <https://doi.org/10.1007/s11046-017-0139-3>.
 48. Souza JAM, de Matos Baltazar L, Carregal VM, Gouveia-Eufrazio L, de Oliveira AG, Dias WG, Campos Rocha M, Rocha de Miranda K, Malavazi I, de Assis Santos D, Frézard FJG, da Gloria de Souza D, Teixeira MM, Soriani FM. 2019. Characterization of *Aspergillus fumigatus* extracellular vesicles and their effects on macrophages and neutrophils functions. *Front Microbiol* 10:2008. <https://doi.org/10.3389/fmicb.2019.02008>.
 49. Kurucz V, Krüger T, Antal K, Dietl A-M, Haas H, Pócsi I, Kniemeyer O, Emri T. 2018. Additional oxidative stress reroutes the global response of *Aspergillus fumigatus* to iron depletion. *BMC Genomics* 19:357. <https://doi.org/10.1186/s12864-018-4730-x>.
 50. Semighini CP, Harris SD. 2008. Regulation of apical dominance in *Aspergillus nidulans* hyphae by reactive oxygen species. *Genetics* 179:1919–1932. <https://doi.org/10.1534/genetics.108.089318>.
 51. Malagnac F, Lalucque H, Lepère G, Silar P. 2004. Two NADPH oxidase isoforms are required for sexual reproduction and ascospore germination in the filamentous fungus *Podospora anserina*. *Fungal Genet Biol* 41:982–997. <https://doi.org/10.1016/j.fgb.2004.07.008>.
 52. Krappmann S, Sasse C, Braus GH. 2006. Gene targeting in *Aspergillus fumigatus* by homologous recombination is facilitated in a nonhomologous end-joining-deficient genetic background. *Eukaryot Cell* 5:212–215. <https://doi.org/10.1128/EC.5.1.212-215.2006>.
 53. Wagener J, Echtenacher B, Rohde M, Kotz A, Krappmann S, Heesemann J, Ebel F. 2008. The putative alpha-1,2-mannosyltransferase AfMnt1 of the opportunistic fungal pathogen *Aspergillus fumigatus* is required for cell wall stability and full virulence. *Eukaryot Cell* 7:1661–1673. <https://doi.org/10.1128/EC.00221-08>.
 54. Helmschrott C, Sasse A, Samantaray S, Krappmann S, Wagener J. 2013. Upgrading fungal gene expression on demand: improved systems for doxycycline-dependent silencing in *Aspergillus fumigatus*. *Appl Environ Microbiol* 79:1751–1754. <https://doi.org/10.1128/AEM.03626-12>.
 55. Hartmann T, Dümig M, Jaber BM, Szewczyk E, Olbermann P, Morschhäuser J, Krappmann S. 2010. Validation of a self-excising marker in the human pathogen *Aspergillus fumigatus* by employing the beta-rec/six site-specific recombination system. *Appl Environ Microbiol* 76:6313–6317. <https://doi.org/10.1128/AEM.00882-10>.
 56. Neubauer M, Zhu Z, Penka M, Helmschrott C, Wagener N, Wagener J. 2015. Mitochondrial dynamics in the pathogenic mold *Aspergillus fumigatus*: therapeutic and evolutionary implications. *Mol Microbiol* 98:930–945. <https://doi.org/10.1111/mmi.13167>.
 57. Hill TW, Kafer E. 2001. Improved protocols for *Aspergillus* salt stock solutions. *Fungal Genet News* 48:20–21. <https://doi.org/10.4148/1941-4765.1173>.
 58. Monteiro MC, de la Cruz M, Cantizani J, Moreno C, Tormo JR, Mellado E, De Lucas JR, Asensio F, Valiante V, Brakhage AA, Latgé J-P, Genilloud O, Vicente F. 2012. A new approach to drug discovery: high-throughput screening of microbial natural extracts against *Aspergillus fumigatus* using resazurin. *J Biomol Screen* 17:542–549. <https://doi.org/10.1177/1087057111433459>.
 59. Basenko EY, Pulman JA, Shanmugasundram A, Harb OS, Crouch K, Starns D, Warrenfeltz S, Aurrecochea C, Stoekert CJ, Kissinger JC, Roos DS, Hertz-Fowler C. 2018. FungiDB: an integrated bioinformatic resource for fungi and oomycetes. *J Fungi (Basel)* 4:39. <https://doi.org/10.3390/jof4010039>.
 60. Engel SR, Dietrich FS, Fisk DG, Binkley G, Balakrishnan R, Costanzo MC, Dwight SS, Hitz BC, Karra K, Nash RS, Weng S, Wong ED, Lloyd P, Skrzypek MS, Miyasato SR, Simison M, Cherry JM. 2014. The reference genome sequence of *Saccharomyces cerevisiae*: then and now. *G3 (Bethesda)* 4:389–398. <https://doi.org/10.1534/g3.113.008995>.
 61. Skrzypek MS, Binkley J, Binkley G, Miyasato SR, Simison M, Sherlock G. 2017. The *Candida* Genome Database (CGD): incorporation of Assembly 22, systematic identifiers and visualization of high throughput sequencing data. *Nucleic Acids Res* 45:D592–D596. <https://doi.org/10.1093/nar/gkw924>.
 62. Waterhouse AM, Procter JB, Martin DMA, Clamp M, Barton GJ. 2009. Jalview version 2—a multiple sequence alignment editor and analysis workbench. *Bioinformatics* 25:1189–1191. <https://doi.org/10.1093/bioinformatics/btp033>.
 63. Pontecorvo G, Roper JA, Hemmons LM, Macdonald KD, Bufton AWJ. 1953. The genetics of *Aspergillus nidulans*. *Adv Genet* 5:141–238. [https://doi.org/10.1016/s0065-2660\(08\)60408-3](https://doi.org/10.1016/s0065-2660(08)60408-3).
 64. Misslinger M, Lechner BE, Bacher K, Haas H. 2018. Iron-sensing is governed by mitochondrial, not by cytosolic iron-sulfur cluster biogenesis in *Aspergillus fumigatus*. *Metallomics* 10:1687–1700. <https://doi.org/10.1039/c8mt00263k>.
 65. Oberegger H, Schoeser M, Zadra I, Abt B, Haas H. 2001. SREA is involved in regulation of siderophore biosynthesis, utilization and uptake in *Aspergillus nidulans*. *Mol Microbiol* 41:1077–1089. <https://doi.org/10.1046/j.1365-2958.2001.02586.x>.
 66. Staib F, Mishra SK, Rajendran C, Voigt R, Steffen J, Neumann KH, Hartmann CA, Heins G. 1980. A notable *Aspergillus* from a mortal aspergilloma of the lung. New aspects of the epidemiology, serodiagnosis and taxonomy of *Aspergillus fumigatus*. *Zentralbl Bakteriol A* 247:530–536.
 67. Schrettel M, Bignell E, Kragl C, Joechl C, Rogers T, Arst HN, Haynes K, Haas H. 2004. Siderophore biosynthesis but not reductive iron assimilation is essential for *Aspergillus fumigatus* virulence. *J Exp Med* 200:1213–1219. <https://doi.org/10.1084/jem.20041242>.